

UC Davis

UC Davis Previously Published Works

Title

Flood-driven topographic changes in a gravel-cobble river over segment, reach, and morphological unit scales

Permalink

<https://escholarship.org/uc/item/8h51s2wh>

Authors

Pasternack, Gregory B
Wyrick, Joshua R

Publication Date

2016-10-11

DOI

10.1002/esp.4064

Data Availability

The data associated with this publication are available upon request.

Peer reviewed

1 Title: Flood-driven topographic changes in a gravel-cobble river over segment, reach,
2 and morphological unit scales

3

4 Short title: Fluvial response to large flood

5

6 Authors: Gregory B. Pasternack^{*a} Joshua R. Wyrick^b

7

8 ^a University of California, Davis, One Shields Drive, Davis, CA, 95616

9 ^b Lafayette College, 740 High Street, Easton, PA, 18042

10

11 * Corresponding author. gpast@ucdavis.edu

12

13 **Keywords:** topographic change; DEM differencing; river morphology; regulated rivers;
14 geomorphic change

15

16 Citation: Pasternack, G. B., and Wyrick, J. R. 2016. Flood-driven topographic changes

17 in a gravel-cobble river over segment, reach, and morphological unit scales. Earth

18 Surface Processes and Landforms, doi: 10.1002/esp.4064.

19

20 **Abstract**

21 Regulated rivers generally incise below dams that cut off sediment supply, but
22 how that happens and what the consequences are at different spatial scales is poorly
23 understood. Modern topographic mapping at meter-scale resolution now enables
24 investigation of the details of spatial processes. In this study, spatial segregation was
25 applied to a meter-scale raster map of topographic change from 1999 to 2008 on the
26 gravel-cobble, regulated lower Yuba River in California to answer specific scientific
27 questions about how a decadal hydrograph that included a flood peak of 22 times
28 bankfull discharge affected the river at segment, reach, and morphological unit scales.
29 The results show that the river preferentially eroded sediment from floodplains
30 compared to the channel, and this not only promoted valley-wide sediment evacuation,
31 but also facilitated the renewal and differentiation of morphological units, especially in
32 the channel. At the reach scale, area of fill and mean net rate of elevational change
33 were directly correlated with better connectivity between the channel and floodplain,
34 while the mean rate of scour in scour areas was influenced by the ratio of slope to
35 bankfull Froude number, a ratio indicative of lateral migration versus vertical
36 downcutting. Hierarchical segregation of topographic change rasters proved useful for
37 understanding multiscale geomorphic dynamics.

38

39 **Introduction**

40

41 Quantification of changes in river morphology provides a means for monitoring
42 rates and directions of landform change relevant to ecosystem services and human

43 activities (Ferguson and Ashworth, 1990; Wheaton et al., 2010b). Although landform
44 change is naturally driven by tectonic and climatic processes (Hack, 1960; Tucker and
45 Slingerland, 1997), there may also be a dominant role for land use (Trimble *et al.*, 1987;
46 Pasternack *et al.*, 2001; Warrick and Rubin, 2007) and the damming of rivers (Williams
47 and Wolman, 1984; Brandt, 2000) in the industrial era of human civilization.

48 Observational studies of these problems in the 20th century used a range of techniques
49 (often together) with different kinds of sampling strategies and limitations (Lawler,
50 1993), including (i) historic map and aerial photo interpretation with spot measurements
51 (Hadley and Schumm, 1961), (ii) intensive planimetric surveys of small sites with limited
52 extrapolative capability (Ferguson and Ashworth, 1992; Valle and Pasternack, 2006),
53 (iii) rapid reconnaissance of qualitatively evaluated metrics (Thorne, 1998), or (iv)
54 statistical analysis of a small sampling of cross-sections (Leopold *et al.*, 2005), with
55 locations distributed based on expert judgment depending on the scale of problem at
56 hand. In the last 20 years, diverse, cost-effective technologies have been developed for
57 meter-scale topographic mapping and fluvial remote sensing over hundreds of
58 kilometers of river length (e.g., Fonstad *et al.*, 2013; Glennie *et al.*, 2013). Processing
59 such vast and complex raw datasets has proven a challenge unto itself (e.g., Drăguț
60 and Eisank, 2011; Mandlbürger *et al.*, 2015; Schaffrath *et al.*, 2015), but it is essential to
61 move forward envisioning what a new paradigm of science and management would look
62 like making use of such data (e.g., Wyrick *et al.*, 2014; Gonzalez *et al.*, 2015; Wyrick
63 and Pasternack, 2015). How do we use meter-scale data to answer fundamental
64 scientific questions about the mechanisms and rates governing fluvial geomorphology

65 and what new understanding can we make with an appreciation of spatial complexity
66 (Passalacqua *et al.*, 2015)?

67 The term 'near-census' is used to describe comprehensive, spatially explicit,
68 process-based approaches using the 1-m scale as the basic building block for
69 investigating rivers. This approach avoids the confounding problems associated with
70 statistical sampling (Gonzalez *et al.*, 2015). The concept of a 'near-census' implies that
71 meter-scale data represents variables in great detail that approaches the population of
72 conditions, but that there remains a finer level of detail in the domain of continuum
73 mechanics that technology already resolves over small areas (Brasington *et al.*, 2012)
74 and will eventually resolve at the landscape scale. Previously, 10-m resolution was
75 recognized as suitable for hillslope analyses (Zhang and Montgomery, 1994; Tarolli and
76 Tarboton, 2006), but for rivers many questions about physical and ecological processes
77 require data and models at submeter to meter resolution.

78 The potential value of near-census data hinges on recognizing that data is not an
79 end to itself, but requires analysis to gain improved scientific understanding over
80 sample-based approaches of the past (Passalacqua *et al.*, 2015). Excluding
81 approaches that use near-census data for numerical model set-up (e.g. Casas *et al.*,
82 2010; Pasternack, 2011) and validation (Williams *et al.*, 2016), new geomorphic
83 analytics are rapidly emerging and generally apply continuum or object-oriented
84 methods. In the former approach, near-census data (point clouds or rasters) are
85 analyzed along continuous profiles or as a 3D surface (e.g., Gangodagamage *et al.*,
86 2007; Lashermes *et al.*, 2007; Booth *et al.*, 2009; Scown *et al.*, 2015; Buscombe, 2016).
87 These methods allow for understanding, even predicting, landscape patterning (e.g.,

88 Legleiter and Kyriakidis, 2008; Perron *et al.*, 2008; Tarolli, 2014), as well as revealing
89 how spatially explicit process variables, such as fluvial hydraulics, are driven by that
90 patterning and in turn promote patterns of sediment erosion and deposition (Brown and
91 Pasternack, 2014). Continuum-based metrics of such process-morphology linkages
92 have even been turned into a topographic design tool for river engineering (Brown *et al.*,
93 2014).

94 Alternatively, and as is employed in this study, near-census data may be
95 segregated into discrete fundamental spatial units of analysis with object-oriented
96 methods, and then the attributes of the units may be compared. A key advantage of
97 segregation and averaging within units is that this avoids the serious problem of spatial
98 autocorrelation when considering individual points or pixels as if they are independent
99 and identically distributed data, which has been neglected in many near-census studies
100 thus far. Herein, no differentiation is made for edge or special-feature
101 detection/extraction, compared to complete data segregation, as these are just
102 presence/absence variations on the more general concept of segregation.

103 Geomorphologists have long divided the landscape into discrete units for a wide variety
104 of reasons and purposes (Evans, 2012), and this practice continues with near-census
105 data. Arguably, this has been the most widespread application of near-census data to
106 date, with dozens of segmentations on the basis of sediment facies, landforms, process
107 domains, inundation thresholds, hydraulics, land use/land cover types, and physical
108 habitat types (e.g., Brennan and Webster, 2006; Brandtberg, 2007; Hauer *et al.*, 2009;
109 Milan *et al.*, 2010; Nelson *et al.*, 2014; Wyrick and Pasternack, 2014, 2015).

110 Segmentation has also been essential for sediment budgeting (e.g., Fuller *et al.*, 2003;
111 Milan *et al.*, 2007; Wheaton *et al.*, 2010a).

112 Fluvial geomorphologists recognize that landforms and processes exhibit multiple
113 spatial scales of organization (Frissell *et al.*, 1986; Grant *et al.*, 1990; Sear, 1994), and
114 as a result have advocated for a multi-scalar, hierarchical approach to understanding
115 and managing rivers (Brierley and Fryirs, 2005; Beechie *et al.*, 2010). In light of near-
116 census developments, multi-scalar frameworks are needed for using near-census data
117 to answer a wide range of multi-scalar scientific questions about rivers, especially about
118 processes that affect rivers and their management, but these do not yet exist. Hay *et al.*
119 (2001) illustrated a multi-scalar approach to addressing terrestrial ecology that involved
120 applying object-oriented analysis to remote sensing data over a range of scales, notably
121 to identify important scales. In fluvial geomorphology many important scales are already
122 known, so the focus is on ascertaining what a multi-scalar framework would involve and
123 what kinds of process-based questions it could answer integrating diverse data inputs.
124 Recently, Wheaton *et al.* (2015) proposed a multi-scalar, near-census framework for
125 mapping landforms, which is an excellent beginning.

126 The overall goal of this study was to apply near-census data and object-oriented
127 analyses within a multi-scalar framework to quantify how topographic changes in a
128 regulated gravel-cobble river are spatially organized at segment (10^2 to 10^3 channel
129 widths, W), reach (10^1 to $10^2 W$), and morphological-unit (10^{-1} to $10^1 W$) scales in
130 response to a hydrologically heterogeneous period that included a flood with an
131 instantaneous peak flow of ~ 22 times bankfull discharge. These scales derive from the
132 widely used system of Frissell *et al.* (1986), who proposed the idea of hierarchically

133 nested scales of analysis in river classification drawing on pre-existing ecological
134 theories about nested scaling. The only common scale not considered in this study is
135 the finest scale termed microhabitat by Frissell et al. (1986) and hydraulic unit by many
136 other systems. This study was motivated by practical management needs and
137 fundamental questions about regulated yet dynamic gravel-cobble rivers, which are a
138 worldwide phenomenon. At the segment scale, when a regulated river has much less
139 downstream sediment supply after regulation than before and somewhat less frequent
140 occurrence of sediment transporting flows after than before (i.e., low S^* and medium T^*
141 *sensu* Grant *et al.*, 2003), then it is going to exhibit a net export of sediment as it
142 evacuates valley-scale sediment storage (Williams and Wolman, 1984), but a key
143 question is whether the channel necessarily disconnects from its floodplain? At the
144 reach scale, are there differences in the amounts of sediment scour and deposition
145 between reaches, and if so what hydraulic processes and geomorphic controls explain
146 them? At the morphological-unit scale, does an incising regulated river necessarily lose
147 differentiation between unit types (perhaps because of flow homogeneity) or may local
148 factors promote renewal of units even as the river loses elevation? In light of natural
149 fluvial heterogeneity and spatial patterning in landforms and processes, these questions
150 are best answered by collecting repeat surveys of near-census data over a long river
151 segment and aggregating the data to the correct spatial scale for each analysis. The
152 fundamental scientific questions explored in this study illustrate the merits of a multi-
153 scalar framework for not only mapping landforms, but also analyzing how rivers change
154 through time.

155

156 **Study Site**

157

158 The 3480 km² Yuba River is a tributary in the Sacramento River basin flowing
159 from the western slopes of the Sierra Nevada to the confluence with the Feather River
160 at Marysville (Fig. 1). The montane-Mediterranean climate is characterized by cool, wet
161 winters and hot, dry summers (Storer *et al.*, 2004). Heavy flooding can occur in the
162 winter when weather systems driven by the Pacific Ocean El Niño Southern Oscillation
163 produce warm rain-on-snow events. Spring runoff is dominated by snowmelt during
164 April-June as temperatures warm.

165 Flow coming out of the mountains and into the valley primarily comes from the
166 North, Middle, and South Yuba River tributaries that join a short distance upstream of a
167 high concrete dam (Englebright Dam) and secondarily from the small, regulated
168 tributary Deer Creek. Englebright Dam marks the start of the lower Yuba River segment.
169 It was constructed as a sediment barrier in 1941 to protect the lower Yuba River from
170 further impact associated with the hundreds of millions of tons of sediment blasted off
171 hillsides throughout the watershed during hydraulic gold mining (Gilbert, 1917).
172 Downstream at river kilometer 17.8, Daguerre Point Dam is an 8-m high irrigation
173 diversion structure that creates a slope break and marks the reach-scale transition from
174 net incision upstream to net deposition downstream.

175 The ~ 37.1 km long section between Englebright Dam and the Feather River
176 confluence is termed the Lower Yuba River (LYR). It exhibits a straight to slightly
177 meandering planform geometry, little entrenchment, a cobble-gravel bed, an average
178 channel slope of 0.16%, and an average wetted baseflow width of 59.4 m (Wyrick and

179 Pasternack, 2012). Even though Englebright Dam blocks bedload, the LYR remains a
180 wandering gravel-bed river due to the gravel-cobble-rich hydraulic-mining deposits
181 (James *et al.*, 2009; White *et al.*, 2010). The mean substrate size in the bankfull channel
182 is 0.1 m, with local size decreasing downstream from 0.3 m near Englebright Dam to
183 0.04 m near the mouth.

184 Instantaneous stage-discharge has been continuously recorded on the LYR at
185 two USGS gages: Smartsville near Englebright dam (#11418000), and Marysville near
186 the mouth (#11421000). Wyrick and Pasternack (2012) defined a representative
187 baseflow discharge for research purposes of 24.9 m³/s above DPD and 15.0 m³/s
188 downstream of DPD (accounting for irrigation withdrawals), which is equivalent to ~ 75%
189 daily exceedence probability. The winter flood regime is highly dynamic despite some
190 flow regulation (controlled releases up to 118.9 m³/s by Englebright Dam), with a field-
191 determined bankfull discharge of ~ 141.6 m³/s occurring every ~ 1.25 years and a field-
192 determined floodplain-filling flow of ~ 597.5 m³/s occurring every ~ 2.5 years (Wyrick
193 and Pasternack, 2012). Above this flow the primary exposed alluvial surfaces in the
194 river valley are terraces and artificial “training” berms that isolate the modern river
195 corridor from a high disturbed mining area known as the Yuba GoldFields.

196

197 **Methods**

198

199 Experimental Design

200

201 An overview of the experimental design is laid out, and then methodological
202 details are presented in the following subsections. Spatial object-oriented analysis of
203 rivers may be delineated according to patterns that are arranged longitudinally and
204 laterally relative to the flow direction in a river. This study evaluated fluvial processes
205 associated with a large flood at three spatial scales using such methods. Data used
206 consisted of (i) topographic digital elevation models (DEMs) of the same river segment
207 in 1999 and 2006-2008 (Carley *et al.*, 2012) and (ii) polygons delineating different
208 landform features at three spatial scales of interest (Wyrick *et al.*, 2012, 2014). At the
209 largest scale, the river valley for the entire LYR was mapped as a single polygon by
210 hand, guided by aerial photography and DEMs (Fig. 2). At this scale, laterally discrete
211 but longitudinally continuous landforms in a river corridor relate to the hydrologic regime
212 necessary to inundate different topographic levels, such as bankfull, floodplain, and
213 terraces. In this study, only two inundation regions were considered- within the bankfull
214 channel and the overbank region. At the next scale down, longitudinally discrete
215 landforms were delineated in terms of geomorphic reaches that spanned the valley's
216 width. Finally, at the smallest scale, morphological units (MUs) ranging in size from ~
217 0.3 to 10 channel widths were mapped on the basis of 2D baseflow hydraulics
218 computed with a numerical model and other landform indicators, as explained below. At
219 each spatial scale, area of each topographic change type (i.e. no detectable change,
220 scour, or fill), net volumetric change, and mean depth of topographic change were
221 computed for each segregating unit (i.e. whole segment, in-channel or overbank,
222 geomorphic reach, and MU type). This allowed for comparison of these variables
223 between the different regions of interest at each spatial scale. Given only six reaches,

224 correlation and regression analyses were challenging, but were undertaken to look for
225 reach-scale landform variables that might explain the differences in topographic change
226 metrics. Topographic change maps were used to interpret regression results. As longer
227 segments are analyzed in the future, this approach will become more statistically robust,
228 so it is worthwhile to pioneer the concept.

229

230 Data

231

232 Survey and DEM data

233

234 Two topographic DEM datasets spanning the downstream-most 34 km of the
235 lower Yuba River (i.e., from the onset of Timbuctoo Bend to the mouth, Fig. 2) were
236 compared to create a detailed map of the areal and vertical changes in topography in
237 response to a hydrologically heterogeneous period that included a flood with a peak
238 daily flow of 2384 m³/s and an instantaneous peak of 3206 m³/s on the Marysville gage.
239 Complete details of the methodology, including spatially explicit uncertainty analysis,
240 are available in Carley *et al.* (2012), but are summarized herein. This study applied the
241 existing data to address new, specific scientific questions about topographic change
242 and sediment budgets, making a new contribution.

243 In 1999, topographic and bathymetric survey data were collected by contractors
244 for the US Army Corp of Engineers to yield a 0.6-m contour map of the LYR.

245 Topographic contours and available point data were combined to produce a 1.5 x 1.5
246 m² (5 x 5 ft²) raster DEM in the State Plane California Zone II (feet) coordinate system

247 (NAD83 datum), with the elevations updated from the original NGVD29 datum to the
248 modern NAVD88 datum. A more recent topographic map of the LYR was produced
249 between 2006 and 2008 (with negligible amount of surveying in 2009) during an
250 extended dry period through a phased effort based on iterative assessment of map
251 quality. Timbuctoo Bend Reach was mapped in 2006, whereas the other reaches were
252 mapped in 2008. Subsequent analyses that hinge on the duration between topographic
253 maps from section to section of river accounted for different epochs for different areas.
254 Additionally, areas of data gaps within each map (especially from areas avoided in the
255 1999 mapping campaign) and known man-made alterations (e.g., mining pits and
256 dredging spoils) between mapping efforts were removed from both DEMs before
257 differencing.

258 The 1999 contour map is a dataset that was provided to the authors as is. For
259 the 2006-2008 surveys, the authors had more control of the survey methods and map
260 production. For this latter DEM, a comprehensive set of uncertainty analyses was
261 performed to ensure that the multiple surveys used to create the single map were
262 accurate and comparable. Ground points on the uneven natural surface were compared
263 between ground-based and boat-based surveys, ground-based and LIDAR surveys,
264 and boat-based and LIDAR surveys. Surveys were also compared at carefully surveyed
265 water surface elevation locations along the water's edge, where surface variability was
266 less. Vertical datums were checked between survey methods. Overall, mean survey
267 differences between methods were within the river's mean grain size (0.1 m). A
268 thorough uncertainty assessment was reported by Barker (2010). A final set of TINs
269 were produced spanning the entire LYR corridor.

270

271 DEM difference map

272

273 Carley *et al.* (2012) undertook an extensive analysis of uncertainty for each DEM

274 and in the combination between the two to identify the best methods for this data set.

275 No longitudinal trend in deposition or erosion was present, so there was no need for

276 continuous longitudinal detrending. Thirteen different approaches for removing

277 uncertain changes cell-by-cell were tested. Given any Level-of-Detection (LoD) raster

278 combining the survey and interpolation errors of each individual DEM, one can either

279 subtract the LoD raster from the DEM difference raster or keep the same differences,

280 but exclude any cell whose LoD exceeds its DEM difference, so Carley *et al.* (2012)

281 tested the effects of both options. For exclusion, five different types of LoDs were

282 evaluated, consisting of different levels of statistical significance for spatially distributed

283 uncertainty and/or excluding the uniform half-contour interval of the 1999 data (i.e., 0.3

284 m). Note that with a 0.1-m mean grain-size in the river corridor, removal from

285 geomorphological consideration of changes that are less than three grains thick is

286 sensible for this quality of data. It is a common problem in current DEM difference

287 studies with near-census data that thin sheets of erosion and deposition cannot be

288 resolved. Spatially distributed uncertainty was computed by evaluating point density and

289 elevation variability within each cell, building on the method of Heritage *et al.* (2009).

290 For subtraction, the same five LoDs were evaluated, and an additional three were also

291 tested in which the spatially distributed LoD was subtracted and then afterwards the

292 uniform 0.3-m half-contour interval LoD was applied as an exclusion. This uniform

293 exclusion is identical to a uniform subtraction of 0.3 m for values within 0.3 m because it
294 removes the values either way, but it retains higher values of change to keep them as
295 they were observed after spatially distributed LoD subtraction. Of the thirteen
296 approaches, the one that was found to perform best involved subtracting the spatially
297 distributed 95% confidence level LoD raster and then excluding the uniform 0.3-m half-
298 contour interval raster. A summary workflow for the final, best Carley *et al.* (2012)
299 method using ArcGIS 10.0 is presented in Figure 3.

300 The final DEM difference map accounting for uncertainty represents the net
301 change in topographic elevation over the 7- or 9-year epoch for each pixel. Any
302 ephemeral topographic changes that occurred between the two map dates but did not
303 persist until the second survey cannot be accounted for with this methodology, which is
304 a long-standing constraint on the repeat survey approach (Horne and Patton, 1989;
305 Lindsay and Ashmore, 2002). The final DEM difference map was reclassified into a
306 presence/absence map of no detectable change, scour, or fill (Fig. 4), which was used
307 to compute the area of each of these categories within different regions.

308

309 Channel and overbank regions

310

311 To evaluate topographic change and sediment budgets for the whole LYR
312 differentiating between in-channel versus overbank regions, ideally there would exist an
313 inundated area map for exactly bankfull discharge in 1999, but no such map or aerial
314 photo exists for the LYR. One solution would be to reconstruct planform channel regions
315 at the same discharge using a hydrodynamic model. In this case that was infeasible,

316 because there were enough DEM data gaps in key locations of the 1999 map to inhibit
317 2D modeling of the river segment. Instead, the approach taken was to use aerial
318 imagery from 1999 when flow was reasonably close to bankfull discharge. Specifically,
319 a wetted area polygon was hand digitized using 0.3-m resolution greyscale aerial
320 imagery collected by Towill, Inc. on April 14, 1999 when the USGS streamflow record
321 indicates a mean daily discharge of $109 \text{ m}^3/\text{s}$ at the Smartsville gage (Fig. 2).

322

323 Geomorphic reaches

324

325 A geomorphic reach is a longitudinally distinct section of river with a
326 characteristic set of attributes controlled by the balance of sediment transport capacity,
327 sediment supply, topography, and possibly other factors such as geology, vegetation,
328 and artificial structures and modifications. On the LYR these governing factors were
329 evident in the following variables: confluences with two major tributaries contributing
330 significant water and some sediment supplies during channel-altering flows, presence
331 and impacts of two dams, degree of lateral confinement of the river-corridor by natural
332 valley slopes and artificial berms, and aspects of the longitudinal profile, including bed
333 slope, slope breaks, and bed undulation pattern. Major changes in these variables were
334 used to delineate six distinct reaches (~ 25-80 channel widths long) in the alluvial LYR,
335 and then numerous topographic change variables were computed at the reach scale to
336 go along with previously determined geomorphic variables from companion studies
337 (Table 1).

338

339 Morphological units

340

341 River landforms, referred to as channel units (appropriate only when within the
342 bankfull channel), geomorphic units, or morphological units, are commonly mapped at a
343 scale of ~ 0.5 to 10 channel widths and are considered to be the basic building blocks of
344 fluvial morphology (Grant *et al.*, 1990; Wadeson, 1994; Wheaton *et al.*, 2015). Wyrick *et*
345 *al.* (2012, 2014) developed a new concept and approach for mapping in-channel
346 landforms at this scale on the basis of how they steer two-dimensional hydraulics at a
347 representative base flow at which the landform dominates hydraulic expression. Using
348 this approach, Wyrick and Pasternack (2014) mapped and analyzed the in-channel
349 morphological units for the whole LYR, including a supplementary file containing the MU
350 map of the whole river over several pages. In addition, Wyrick and Pasternack (2012)
351 mapped overbank morphological units on an expert basis drawing on many spatially
352 explicit geospatial indicators from geomorphic datasets and two-dimensional
353 hydrodynamic modeling of floods performed by Abu-Aly *et al.* (2013). Considering both
354 in-channel and overbank landforms a total of 27 distinct alluvial MU types were
355 identified, described, and mapped. This MU map was used for segregating topographic
356 change and computing sediment budgets in this study. The assemblage of MUs varied
357 by reach (Fig. 5). For example, among the 8 in-channel bed units, the wetted area of
358 Timbuctoo Bend Reach had 20.2 % pools and 18.4% riffles, that for the Daguerre Point
359 Dam Reach had 5.2% pools and 13.6% riffles, and that for the Marysville Reach had
360 52.2% pools and 2.2% riffles. In the bank region, the wetted area of Timbuctoo Bend

361 had 15% medial bar, while that for the Daguerre Point Dam Reach had 1.5% medial
362 bar.

363 As previously mentioned, surveying data gaps in 1999 precluded 2D
364 hydrodynamic modeling and MU mapping of the LYR, so this study cannot address the
365 fate of MUs during a flood, which is an important question for future inquiry. Instead,
366 MUs were mapped for the 2006-2008 DEM, so this study was able to assess the
367 topographic changes that drove their formation and/or rejuvenation. This enables the
368 study to answer whether the LYR maintains a strong differentiation between MUs after a
369 flood, which is an equally important question.

370

371 Analysis Methods

372

373 Area, volume, and mean depth

374

375 At each spatial scale, area of each topographic change type (i.e. no detectable
376 change, scour, or fill), net volumetric change, and mean depth of topographic change
377 were computed for each segregating unit (i.e. whole segment, channel region, reach, or
378 MU type). The final spatially explicit, uncertainty-adjusted DEM difference map provided
379 a net change in elevation for each $1.524 \times 1.524\text{-m}^2$ ($5 \times 5\text{-ft}^2$) pixel, so the volume of
380 change within each was simply this value times the area of the pixel (2.323 m^2 , 25 ft^2).

381 For each scale of analysis, these pixel volumes were then summed within the

382 appropriate segregating unit.

383 Uncertainty in volumetric change estimation from DEM difference data is a highly
384 challenging topic with no clear method outshining others, or none at all. In common
385 statistics, one would normally compute the raw mean volume and then apply uncertainty
386 bands (computed through repetition) around that, which in this case might be the
387 volume of the 95% confidence LoD for any given area. However, in DEM difference
388 studies the raw mean elevational value in each cell is known to be uncertain, so it
389 should not be used to compute the expectation for the mean volumetric change. For
390 example, in this study, the net volumetric change of the raw DEM difference was a fill of
391 $1.20 \times 10^5 \text{ m}^3$, which is impossible given that the river segment begins at a high dam
392 and there is virtually no other sediment influx, so the net change has to be negative
393 (Carley *et al.*, 2012). Thus, an elevational correction has to be applied before the
394 expected volume is computed, but then what is the appropriate variance around the
395 adjusted number as opposed to that for the raw number? It is probably not the same
396 thing, as the distribution of DEM difference values changes after adjustment, but there
397 is no method to account for this yet. As an example of an aggressive volumetric
398 uncertainty approach, Wheaton *et al.* (2013) began with a raw DEM difference raster
399 and then subtracted the 95% confidence LoD raster from it, similar to what was done in
400 this study. They then computed volumes the same way as proposed in the preceding
401 paragraph and termed those the “mean estimate” of change, but clearly this is the
402 adjusted mean, not the raw mean. To get some measure of volumetric uncertainty, they
403 then computed a new LoD for the raw DEMs using the 68% confidence level, and
404 computed volumes for areas on that raster. Finally, they considered the volumetric
405 uncertainty around the mean estimate for any area to be the corresponding volume of

406 the 68% confidence level LoD in that same area. That assumes that the variance
407 around the adjusted volumes is identical to that around the raw ones. Overall, this is a
408 double counting of the same elevational uncertainty in the raw DEMs, rather than an
409 independent accounting of elevational and volumetric uncertainty. Wheaton *et al.* (2013)
410 showed evidence that this is an excessive loss of real change, but the tendency is to
411 want to do something. Further complicating matters is the fact that there are significant
412 differences in the datasets people have in different studies, making the best method of
413 volumetric uncertainty accounting uncertain. Thus, technically sound and scientifically
414 meaningful approaches for spatially explicit volumetric uncertainty analysis (on top of
415 elevational uncertainty analysis) in different settings are presently unreliable, so no such
416 procedure was used in this study.

417 Due to different time epochs measured for different regions of the river, the
418 volumetric analyses presented are in units of volume per year, thus enabling easier
419 comparisons among all river regions and spatial scales. For scales that transcend
420 different time epochs, the river was segregated into regions of each time epoch, and
421 then the annual rates were calculated for each epoch region and summed for the whole
422 segment. The time epoch was seven years (1999-2006) for Timbuctoo Bend and nine
423 years (1999-2008) everywhere else.

424 Mean depths of topographic change were calculated by dividing each net
425 volumetric change by total area of a segregating unit. Additionally, mean depths of
426 change were isolated for only those regions that experienced scour or fill (i.e., the net fill
427 volumes were only divided by the net fill planform areas, and likewise for the net scour,
428 within the segment, reach, or MU scales). These stratifications highlight how much

429 dynamism occurred within certain regions as compared to the overall net depth changes
430 at each spatial scale.

431

432 Segment scale methods

433

434 Four analyses of topographic change were performed considering the river
435 segment as a whole. Recall that the guiding question posed in the introduction was to
436 ascertain whether regulated river incision would disconnect the channel from the
437 floodplain, which is a common concern for regulated rivers (Williams and Wolman,
438 1984; Brandt, 2000). First, aggregate statistics of topographic change volumes and
439 depths were computed. A reclassified DEM difference raster was used to obtain the
440 overall area of each category of topographic change. Second, topographic changes
441 were segregated by channel region (i.e., in-channel versus overbank) to determine the
442 extent to which topographic change intensified channel-floodplain separation or
443 ameliorated it. Third, the segment was divided longitudinally into two areas on the basis
444 of being above or below the run-of-the-river dam, Daguerre Point Dam, to determine
445 how it was affecting erosion and deposition at the segment scale.

446 Finally, longitudinal profiles in topographic change were assessed to look for
447 secular trends at the segment scale. To analyze the longitudinal trend, the relative area
448 of each change class was determined within discrete, contiguous cross-sectional
449 rectangles. To accomplish this, a centerline was drawn for the valley polygon, which
450 was then stationed every 6.1 m (20 ft). From these station points, perpendicular lines
451 were extended out to the valley boundary and then buffered 3 m (10 ft) in both the

452 upstream and downstream direction, thus creating a continuous coverage of the valley
453 area with cross-sectional rectangles (Wyrick and Pasternack, 2012). The areas of each
454 change class within each rectangle were then calculated in ArcGIS, with the areas
455 being assigned to the longitudinal station of each rectangle. These areas were then
456 converted into percent of total area at each station to create a longitudinal profile that
457 highlights the spatial patterns of areal dominance/subordinance of each change class.

458

459 Reach scale methods

460

461 To analyze topographic change at the reach scale, the same approach as was
462 used for the segment-scale channel regions was used, but this time geomorphic reach
463 polygons were the segregating boundaries. Two broad topics were addressed at the
464 reach scale. First, this is the appropriate scale to perform a longitudinal sediment
465 budget. Second, statistical analyses were done to see if any hydrogeomorphic variables
466 related to metrics of reach-scale topographic change patterns.

467 A sediment budget is an accounting of inorganic particulate mass fluxes and
468 abundances within an established control volume for a specified time period. In this
469 study, the segment-scale control volume is the LYR valley and the sediment budget
470 involves the flux and storage of sediment among the reaches within the segment. Apart
471 from turbid mud suspended in the water column as wash load and a few very small
472 tributaries, there is negligible influx of sediment into the LYR valley, because
473 Englebright Dam blocks influx. Both gaged tributaries (Dry and Deer Creeks)
474 downstream of the dam are themselves dammed and Deer Creek is almost purely

475 bedrock downstream of its dam. Dry Creek likely does export some sediment to the
476 LYR, which may explain the broadening that occurs just downstream of its confluence.
477 A volumetrically small influx of boulders and angular rock fractured off the bedrock-soil
478 interface occurs where the perennial channel is against the hillside. In contrast, the
479 valley floor stores on the order of ~ 100 million cubic meters of hydraulic-mining
480 alluvium (Gilbert, 1917; James, 2005; James *et al.*, 2009, 2010). As a result, the
481 sediment budget for this control volume is greatly simplified and consists of net export
482 equaled by a volumetric loss of sediment storage.

483 Despite the simplicity of the sediment budget, there are still sources of
484 uncertainty and a need to be clear about what is accounted for and what is not. First,
485 similar to areal analysis, the volumetric sediment budget can only discern and quantify
486 volumetric changes in which there is a net change within a cell. If a cell erodes and then
487 fills back in all within the re-survey time domain, then no change will be detected in that
488 cell- a process known as compensating scour and fill (Lindsay and Ashmore, 2002). If
489 the sediment came from an upstream cell within the control volume, then the change
490 would be detected in both; however, the two volumes will not be spatially linked (i.e., we
491 cannot determine which sediment moves to where).

492 Second, it is assumed that there are no non-transport mechanisms of volumetric
493 change (i.e. bed “deflation” or “inflation”). Merz et al. (2006) reported that gravel-
494 placements sites experienced up to 20% volumetric loss (i.e., deflation). Marquis and
495 Roy (2012) reported that a gravel bed may undergo “dilation” or “contraction”
496 (analogous to inflation and deflation in Merz et al. (2006)) due to injection or loss of finer
497 particles from the bed during a state of partial transport. In the case of the LYR, there

498 were no gravel-placement projects and the bed had two years to deflate and adjust after
499 the significant 1997 flood. Nevertheless, there is uncertainty caused by unknown
500 mechanisms of non-transport and partial transport deflation/contraction and
501 inflation/dilation.

502 Beyond evaluating the sediment budget, statistical analysis was used to
503 investigate what hydrogeomorphic controls explained differences in the amounts of
504 sediment scour and deposition between reaches. Drawing on the data in Table 1, binary
505 correlations were calculated between topographic change metrics and potential
506 controlling variables. For those showing statistically significant results in terms of high
507 correlation coefficients and low p-values, regression analysis was done to inspect the
508 relation to see if the results were scientifically meaningful. Also, topographic change
509 maps of example sites are presented for visual corroboration of the interpreted
510 geomorphic mechanism.

511

512 Morphological unit scale methods

513

514 To analyze topographic change that drove the pattern of MUs, the same
515 approach as was used for the segment-scale channel regions was used, but this time
516 the boundaries used to segregate the area, volume, and depth data were the MU
517 polygons. The key test was whether areas that became different MU types exhibited
518 similar or differential topographic changes. Further, if the river and valley are
519 downcutting, did all landforms necessarily decrease? Sorted column plots were used to

520 visualize MU-specific volumes and depths of change on an annualized basis, again
521 accounting for the two different epochs in the study as described earlier.

522

523 **Results**

524

525 Segment Scale Results

526

527 Aggregate changes

528

529 For 1999 to 2008, the LYR exhibited massive internal changes in topography
530 (Fig. 4), yet had a very small net loss of sediment from the river corridor. In terms of
531 area, 46.7% of the total area experienced no detectable change, while 31.0% filled and
532 22.3% scoured. The annualized scour and fill volumes were $2.93 \times 10^5 \text{ m}^3/\text{yr}$ (51.5% of
533 total change) and $2.76 \times 10^5 \text{ m}^3/\text{yr}$ (48.5%), respectively, which means a net annual
534 export of $1.70 \times 10^4 \text{ m}^3/\text{yr}$. The mean rate of depth change for the full valley width was a
535 net scour of 1.8 mm/yr. By stratifying the segment into regions of either net scour or net
536 fill, the dynamism of the processes are better exhibited. In scour areas, there was a net
537 downward elevation change of 13.5 cm/yr, while in fill areas there was a net upward
538 elevation change of 9.1 cm/yr. Thus, even though fill processes covered more total
539 planform area, scour processes moved more volume of sediment and caused more
540 elevation change. These results make sense, because there is nearly zero influx of
541 sediment due to Englebright Dam, so a net fill result would be physically impossible.
542 Further, the river experienced a large flood between surveys, as well as several small to

543 moderate magnitude floods. This indicates that there was ample transport capacity
544 during the study epoch to create diverse local changes and induce a net sediment
545 export out of the river.

546

547 In-channel versus overbank

548

549 When the segment was stratified into in-channel and overbank regions, it was
550 revealed that the latter were as dynamic as the former. The in-channel region had no
551 detectable change for 49.5% of its area, while the overbank region had that for 46.0% of
552 its area. Slightly more in-channel area experienced scour than did overbank area
553 (24.1% versus 21.5%), while the overbank region experienced more area of fill (32.5%
554 versus 26.4%). Considering change volumes, the opposite was found as for area, with
555 in-channel region experienced net fill, while the overbank region experienced net scour.
556 The 1999 near-bankfull wetted channel region experienced a net fill rate of 5.8 mm/yr as
557 the channel migrated to its 2006-2008 location. The overbank regions experienced a net
558 scour rate of 3.8 mm/yr. This indicates that as the channel migrated to the 2006-2008
559 location, it tended to fill in its old channel, scour through the banks, and cut new
560 pathways over floodplains.

561 The overbank net scour rate can be attributed to both the fact that the wetted
562 channel migrated through the floodplain, eroding out a new channel, and that overbank
563 floods provide enough transport capacity to erode the floodplains. The in-channel net fill
564 rate can be attributed to the fact that as the channel migrated, its old channel regions
565 became depositional zones for the overbank flows, thus effectively filling them in.

566

567 Longitudinal changes

568

569 The LYR shows a distinct downstream scour and fill trend in which there are
570 three zones with a predominance of scour and two with a predominance of fill (Fig. 6).
571 The results for this analysis were similar for area, volume, and depth of change. Most of
572 the scour tended to occur upstream of DPD, with the most occurring in the upper ~ 6 km
573 of the study segment. That section experienced a net annual scour rate of 4.48×10^4
574 m^3/yr . The scour zone in this upstream area is explained by valley constriction and
575 “hungry water” in which over-dam floods have significant sediment transport capacity
576 but no supply due to the dam, so sediment stored at the head of the valley is entrained.

577 The rest of the LYR valley above DPD experienced a net scour rate of 5.44×10^4
578 m^3/yr , for a total annual scour rate of $9.92 \times 10^4 \text{ m}^3/\text{yr}$ above DPD. The maximum local
579 net scour rate was 28 cm/yr and occurred just upstream of DPD. The zone of scour
580 upstream of DPD is interpreted to be due to the 1997 flood depositing excessive
581 sediment in this zone followed by the 2006 flood scouring that material out. This is
582 professional interpretation, but it is known from direct experience and management
583 activities that the accommodation space upstream of DPD was full of sediment prior to
584 the 2006 flood and had no additional storage capacity. The maximum relative areas of
585 fill occurred upstream of the Dry Creek confluence, and near the downstream end of the
586 Daguerre Alley training berm. These are both areas that experience backwater effects
587 and are very wide compared to the rest of the river corridor.

588 The region of the LYR below DPD experienced a net annual fill rate of 8.22×10^4
589 m^3/yr . The maximum local fill rate was 11.3 cm/yr and occurred where an overflow
590 anastomosing channel re-connects to the mainstem river. It is interesting that the river is
591 filling in downstream of DPD and scouring above it, as this is the exact opposite of the
592 conventional wisdom of the effects of dams. The reason is that these processes are not
593 being driven by the dam, but rather the river is driven by larger forces of sediment
594 redistribution associated with valley recovery to the end of hydraulic mine sediment
595 being delivered since Englebright Dam was built in 1941. The maximum relative areas
596 of fill in the river occurred in areas that experience backwater effects and are very wide
597 compared to the rest of the river corridor. The scour zone at the downstream end is
598 explained by base level drop in the Feather River causing knickpoint retreat through the
599 LYR. Also, levees confine this eroding section, focusing flow to yield high flood
600 velocities.

601

602 Reach Scale Results

603

604 Comparing among the six geomorphic reaches, there were significant differences
605 in relative percent area of scour (11-55%) and fill (10-45%) as well as in mean net rate
606 of change (-5.9 to 1.9 cm/yr), mean scour rate in scour areas (10.3-17.3 cm/yr), and
607 mean fill rate in fill areas (8.6-14.7 cm/yr) (Table 1). Delineating volumetric change by
608 reach, only two, both upstream of DPD, were net scour, while the other four reaches
609 were net fill (Fig. 7). The DPD and Hallwood reaches experienced the most net fill, while
610 the Parks Bar and Marysville reaches experienced relatively small net fill rates. The

611 upstream-most reach, Timbuctoo Bend, experienced scour over 44.5% of its area and
612 fill only over 10.4% (the least relative fill area of all reaches). It is notable that scour was
613 not limited to the channel, but occurred over the whole width of the river corridor in this
614 valley-constricted reach. This reversed in the Parks Bar reach immediately downstream,
615 which experienced much less scour than fill (19.7% and 32.9% of the area,
616 respectively). The Dry Creek reach exhibited the most relative area of scour (55.3%),
617 while the adjacent downstream reach, DPD, exhibited the most relative area of fill
618 (44.9%) among all reaches. The Hallwood and Marysville reaches experienced the
619 smallest areas of detectable change (< 50%, whereas all other reaches had > 50%
620 detectable scour plus fill). Only two of the six reaches exhibited more relative areas of
621 scour than fill (Timbuctoo Bend and Dry Creek), while scour areas were clearly
622 subordinate in the DPD and Hallwood reaches (12% and 11%, respectively). The
623 relative areas of scour and fill are most similar in the Marysville reach, whereas the
624 other reaches can easily be identified as either scour- or fill-dominant.

625 Statistical analysis at the reach scale found that many commonly measured
626 reach-scale variables, especially ones used in river classification, failed to show binary
627 correlations with any of the topographic change metrics at the reach scale. For
628 example, all of the following variables yielded no statistically significant influence:
629 channel sinuosity, channel bed slope, substrate size, bankfull width to depth ratio,
630 specific stream power, mean baseflow width, mean bankfull width, mean floodway
631 width, river valley width (minimum, mean, and maximum), bankfull wetted area, or
632 floodway wetted area. The only statistically significant ($p < 0.02$), high regressions
633 ($r > 0.88$) found to explain topographic change metrics between reaches involved the

634 entrenchment ratio and the ratio of bed slope (S) to bankfull Froude number (Fr_b) (Fig.
635 8). By definition, the entrenchment ratio is the ratio of the width of the valley at an
636 elevation of twice bankfull depth versus the width at bankfull depth (*sensu* Rosgen
637 1996), and thus the higher the value, the less entrenched the channel is. According to
638 the data, channels that are incrementally better connected to their floodplains exhibit
639 incrementally more fill area. On the LYR, the greatest contrast in this process comes
640 from comparing the Daguerre Point Dam Reach with the Timbuctoo Bend Reach. The
641 former has a highly connected channel and floodplain as well as an anastomosing
642 pattern with a secondary channel on the northern flank that activates when flow is
643 between 2-3 times bankfull discharge. This extra secondary channel area preferentially
644 fills. In contrast, Timbuctoo Bend is in a confined valley and scouring throughout the
645 river corridor, so it has little area of fill. Thus, the entrenchment ratio yields a
646 scientifically comprehensible influence over the area of fill. Compared to other potential
647 controlling variables, it shows higher correlations with other topographic change metrics,
648 but none that are statistically significant given only six data points.

649 Meanwhile, the ratio of S/Fr_b showed a relation with the mean scour rate in scour
650 areas (Fig. 8b). In the plot, higher scour is represented by a more negative number, so
651 the effect is a direct correlation, with a higher S/Fr_b corresponding with a higher mean
652 scour rate. The data in this analysis showed one point with a low S/Fr_b , one with a high
653 value, and then four with similar intermediate values, thus it is easiest to interpret by
654 comparing the two extremes. Once again, the Daguerre Point Dam Reach is involved,
655 as it has the highest S/Fr_b , but this time the issue relates to its processes at bankfull
656 flow. The pattern of scour in this reach is easily interpreted as lateral migration, because

657 there is scour at every outer cutbank along the bankfull channel and deposition on each
658 inner point bar (Fig. 9a). This is objectively identifiable in that the area of scour is just
659 outside the 1999 wetted area polygon along the outsides of the meander bends. In
660 contrast, the Marysville reach has the lowest S/Fr_b and its scour is easily interpretable
661 as in-channel downcutting, because it is located predominantly inside the 1999 wetted
662 area polygon, which remained the location of the bankfull wetted area in 2008 (Fig. 9b).
663 Thus, S/Fr_b is revealed to be a controlling variable over the relative roles of lateral
664 migration versus vertical downcutting at the reach scale in the LYR.

665

666 Morphological Unit Scale Results

667

668 There were three MU types that mostly experienced no detectable change -
669 hillside/bedrock, tributary delta, and agriplain, and therefore were more likely to have
670 been the same MU in 1999 and 2008. All other MU types were delineated in regions
671 that experienced significant change. Island high floodplain units were delineated in
672 regions that experienced the most relative area of change (~ 90%), with ~ 82% of those
673 areas altered by fill. Regions that became MU types in which scour was clearly
674 dominant and fill was clearly subordinate, in terms of relative areas, included pool,
675 chute, tributary channel, run, cutbank, and fast glide. For point bar, 67% of its area
676 experienced some detectable change, with ~88% of those areas being fill. This aligns
677 with the unit definition used by Wyrick and Pasternack (2012), who identified point bars
678 as regions of deposition on the inside bank of a river meander.

679 Interpretation of the volumetric changes at the MU scale is the same as
680 discussed for the areal analyses. The reported values are the volumes that scoured or
681 filled into areas that became these delineated landforms (Fig. 10). With that in mind, the
682 floodplain and high floodplain units occurred in areas that experienced the most net fill
683 (5.15×10^4 and $2.85 \times 10^4 \text{ m}^3/\text{yr}$, respectively), while the dredger tailings and pool units
684 in areas that experienced the most net scour (3.47×10^4 and $3.31 \times 10^4 \text{ m}^3/\text{yr}$,
685 respectively). All of the in-channel units were formed by net erosional processes, but
686 they did exhibit significantly different rates amongst themselves.

687 One landform type of geomorphic interest is the swale, which experienced
688 relatively high values of both scour and fill; however, the net volumetric movement is
689 only ~2.5% of the total dynamism. Other unit types of interest are those that constitute
690 the baseflow channel bed – riffle, pool, chute, run, riffle transition, fast glide, slow glide,
691 and slackwater. All the regions that became these units were net scour, with only small
692 portions of their dynamism attributed to fill processes. Riffle transition regions
693 experienced the most volumetric fill (~ 28 % of total volumetric sediment movement),
694 while pool regions experienced the least (~ 1%). Riffles and pools are often
695 complementary end-members in river morphology studies, and are therefore also
696 generally linked as end-members for discharge-dependent transport regimes that
697 describe river “self-maintenance”. Because the regions that ended up as riffles
698 experienced 18% deposition, they appear to have been rejuvenated relative to the
699 regions that ended up as pools, which experienced 99% scour. This contributes to the
700 concept of self-maintenance in the LYR. Nevertheless, it is important to understand that
701 even the places that became riffles at the end of the epoch scoured a lot during the

702 main flood, and thus generally may be interpreted as erosional plateaus rather than
703 depositional bars.

704 Whereas the story at the segment and reach scales are very similar between
705 areal, volumetric, and depth analyses, the MU scale analyses shows some striking
706 differences in the rate of depth changes (Fig. 11) versus the areas and volumetric rates.
707 This is due to the vastly different areas covered by various MU types. For example, the
708 MU-scale regions that exported the most net volume of sediment were those that began
709 and ended as dredger tailings, but their depth of change was middling. Conversely the
710 regions that became cutbank only exported a small volume relative to the other units,
711 but exhibited the greatest local dynamism with a mean scour rate of 16.8 cm/yr.
712 Regions that became pools and chutes were also locally erosive. These units tend to be
713 located near the center of the channel; however, because it is impossible to speculate
714 whether these same pools and chutes existed in the 1999 channel, we cannot with any
715 certainty fully ascribe these high depth change rates to either entrenchment processes
716 or channel migration and the need to carve out deeper locations for its new pools and
717 chutes.

718 At the other end of the processes continuum, regions that became floodplain
719 experienced the most volume of sediment fill, but because this unit was so large, the
720 rate of depth changes was fairly mundane at 2.0 cm/yr (Fig. 11). The most dynamic fill
721 locations were within the regions that became point bar and island high floodplain (both
722 5.4 cm/yr). Thus, during the 7-9 year survey epoch, point bars grew at a faster rate than
723 any other MU type, highlighting the meandering nature of the LYR channel. The fact

724 that island high floodplain and island floodplain units also grew at a higher than average
725 rate highlights the restorative deposition regimes of large floods in the LYR.

726

727 **Discussion**

728

729 Valley fill evacuation

730

731 This study provides new insights into the processes, rates, and patterns of
732 alluvial valley evacuation of sediment at reach and segment scales after dramatic, rapid
733 changes to flow and sediment supply regimes. The LYR valley was first filled in with
734 sediment during a few decades, and then had all further supply stopped by a tall dam.
735 For ~ 70 years the river has been internally redistributing and exporting that material. At
736 this time, terraces and artificial dredger tailing berms from historic anthropogenic
737 disturbances yield visually charismatic erosion, given their height and conspicuousness.
738 They are composed of historic hydraulic mining sediment laden with inorganic mercury
739 (used in historic gold extraction) of concern to downstream biogeochemistry in oxygen-
740 poor aquatic and emergent habitats. However, they are not in fact the major source of
741 sediment (and mercury) that deposits downstream or leaves the system now, or even
742 likely in the next two centuries and possibly the one after that. Singer et al. (2013)
743 speculated that eventually these will be important sources of mercury export, because
744 the valley floor will have achieved equilibrium, but this study shows that it will be in a
745 distant future or may not happen at all, also depending on management decisions.

746 Large floods on the LYR tend to be ~ 2000 to 5000 m³/s, with the largest
747 recorded daily peak flow (1904 to 2015) occurring in December 1964 at an estimated
748 5097 m³/s at the Marysville gage. Such a large flood occurred on December 31, 2005
749 during the epoch investigated, with daily average and instantaneous peak values at the
750 same gage of 2384 and 3206 m³/s, respectively, with a long duration of flow above
751 bankfull stage in the 2006 water year, so this study bears on the issue of mercury export
752 potential. The results found that a large flood has a far greater effect of sediment
753 erosion on the valley floor than from remnant terraces and artificial training berms, but
754 both are contributing to allowing the valley to be exhumed as a whole. Based on
755 interpreting the segment-scale topographic change patterns relative to lateral inundation
756 zones, vertical downcutting in the channel, vertical scour on the floodplain floor, and
757 channel bank migration at the channel-floodplain margin were the primary mechanisms
758 of sediment erosion during this large-flood epoch.

759 Historic sedimentary fill that underlies riverbed and floodplain surfaces at any
760 moment in time will become available to the river as the valley downcuts. Upon
761 inspection through excavation, these materials are well-mixed deposits in terms of
762 particle sizes and composed of the same hydraulic mining sediment, including mercury-
763 laden fine sediment, as in the tailings and terraces, which makes sense as they are all
764 from the same mining sources and deposited in a relatively brief historical period
765 (Pasternack, 2008). Samples taken from the surficial layer of the riverbed are quite
766 different from these underlying sediments and should not be presumed to represent
767 them.

768 Further, Timbuctoo Bend, the upstream-most alluvial reach, was found to be
769 downcutting valley-wide 1999-2006 and was doing so the fastest of all reaches.
770 Considering the net of erosion and deposition, this study found a mean net downcutting
771 rate for the reach's valley alluvium of 4.55 cm/yr during this epoch. Considering only net
772 erosional pixels, the mean downcutting rate in the reach was 13.6 cm/yr. These are fast
773 topographic changes and reflect the capability of a large flood in a constricted valley to
774 access and erode anywhere in the flood zone.

775 To determine how long remains before valley-wide downcutting will cease to
776 dominate erosion and when remnant peripheral terraces in Timbuctoo Bend will be the
777 primary source of sediment, one has to consider the total supply of stored hydraulic
778 mining sediment in this reach above base level. Pasternack (2008) did some simple
779 estimates of the volume of remnant mining sediment in Timbuctoo Bend above the base
780 level at the end of the reach and concluded that there was ~ 6.1-16 million m³, with a
781 best intermediate estimate of 11.9 million m³. Based on the export rate within TBR
782 alone, the remnant mining sediment would be removed in ~ 266 years.

783 Erosion and net export is also occurring in a large quantity downstream of
784 Timbuctoo Bend and upstream of Daguerre Point Dam (a larger area of scour at a lower
785 rate of valley-wide downcutting). Given ~ 100 million cubic meters of hydraulic-mining
786 alluvium and the net export rate 1999-2008, the LYR would need on the order of 6000
787 years to excavate it all, all other things being equal and assuming that the regional base
788 level could be returned to the pre-mining elevation, which is likely impossible.

789 These evacuation estimates provide a rough guideline to what might happen, but
790 heavily depend on the future hydrologic regime and continued presence of dams, which

791 are both uncertain. For example, the future of the ~ 10.3-m high Daguerre Point Dam
792 (that is important for irrigation diversions) is uncertain, with some constituents calling for
793 its removal. If that happened, the valley upstream of it would be evacuated to a much
794 larger depth than the current base level imposed by the dam, and that would take
795 perhaps an additional century (e.g., ~ 10 m thickness divided by ~ 5 cm/yr average
796 scour depth yields 200 additional years to evacuate) or more, depending on
797 unpredictable river management decisions, such as efforts to build valley floor forests
798 that would stabilize existing deposits. Even with speculation about a greater potential for
799 a more aggressive climate producing more large floods than in the past in California
800 (Das et al., 2011; Singer et al., 2013), the valley floor has ample sediment to continue to
801 export well into the future and appears to be currently eroding terraces without a
802 changed climate. Thus, whatever fine sediment and mercury is leaving the LYR, it will
803 be quite a long time, likely beyond two centuries, before the primary concern might be
804 on any remnant terraces, assuming they remain unforested and unprotected in place
805 and are not eroded concomitant with the valley floor as has been happening.

806 Looking beyond the LYR, the remarkable and novel finding that is more universal
807 is that a cobble-gravel river with substantial stored sediment in a confined valley, such
808 as might occur downstream of an alpine glacier, can effect valley-wide downcutting
809 when subjected to flows of > 15 times bankfull discharge every ~ 10 to 20 years. A
810 remarkably small amount of material is being left behind as remnant peripheral terraces.

811

812 Differential rates form MUs

813

814 The guiding scientific question at the MU scale in this study was whether an
815 incising, regulated river loses differentiation between unit types or do local factors
816 promote renewal of units even as the river loses elevation? Highly regulated rivers with
817 negligible sediment supply, little sediment storage, and homogeneous flows are widely
818 known to exhibit a loss in relief. Long durations of low flows keep scour focused on
819 riffles, cutting them down and armoring them, while pools fill in, creating long,
820 homogeneous runs and glides. Flow heterogeneity has previously been shown to be
821 important to morphological diversity in flumes (Parker et al, 2003).

822 This study provides strong field-based evidence that a dynamic flow regime can
823 maintain and enhance MU differentiation, even in the absence of sediment influx, as
824 long as there is adequate sediment in storage for redistribution. Twenty-seven different
825 MU types were present in the LYR at the end of the study period, and the results
826 showed that the final MUs were formed as a result of strongly differential intensities and
827 volumes of topographic change over 7-9 years. In the channel, pools and chutes formed
828 in the places scoured most intensely, while riffles, slow glides, and slackwaters formed
829 in less intensely scoured areas. In the bank region, point bars filled the most, medial
830 bars filled less than half as much, and lateral bars along straightaways scoured. All of
831 these changes are signs of a dynamic, rejuvenating geomorphic regime.

832 Although not explored in this study, two-dimensional hydrodynamic modeling
833 studies by Sawyer et al. (2010) and Abu-Aly et al. (2013) revealed hydraulic
834 mechanisms for the geomorphic processes on the LYR. Flows of ~ 0-2, 2-8, and 8-25
835 times bankfull discharge tended to preferentially scour riffles, pools, and overbank
836 regions, respectively. Thus, each range of flows provides a different geomorphic

837 functionality. From a management perspective, this suggests that environmental flows
838 for geomorphic purposes should not aim for a single peak, but should be varied to drive
839 differential processes.

840

841 **Conclusions**

842

843 This study demonstrated the utility of a multi-scalar approach to segregating
844 meter-scale topographic change data for the purpose of answering different basic
845 scientific questions that each depend on a unique spatial scale. At the segment scale,
846 the LYR is net erosional and its large floods effectively evacuate sediment from the full
847 width of the river corridor. Fill dominated within the channel, whereas scour dominated
848 overbank. Often it is assumed that deposition will occur upstream of a dam and erosion
849 downstream of it, but in this study the opposite was found at a run-of-the-river dam.
850 Effects of a dam need to be evaluated in the local context given the unique history of
851 sediment supply and transport capacity, and not presumed based on idealized dogma.
852 Finally, at the scale of morphological units, the presence of areas with significantly
853 different intensities and volumes of scour and fill was found to produce a diverse array
854 of MUs. Stage-dependent local hydraulics control the occurrence and pattern of
855 differential topographic change, hence the need for variable flow regimes. Overall, near-
856 census topographic change studies are well served by segregating results at multiple
857 scales to investigate different scientific questions.

858

859 **Acknowledgments**

860

861 Primary funding for this study was provided by the Yuba County Water Agency
862 (Award #201016094), the Yuba Accord River Management Team, and the USDA
863 National Institute of Food and Agriculture (Hatch project number #CA-D-LAW-7034-H).
864 We thank the anonymous peer reviewers for helpful comments and editing.

865

866 **References**

867

868 Abu-Aly TR, Pasternack GB, Wyrick JR, Barker R, Massa D, Johnson T. 2013. Effects
869 of LiDAR-derived, spatially-distributed vegetative roughness on 2D hydraulics in
870 a gravel-cobble river at flows of 0.2 to 20 times bankfull. *Geomorphology*.
871 DOI:10.1016/j.geomorph.2013.10.017.

872 Barker JR. 2010. Lower Yuba River QA/QC comparison: LIDAR data, boat echo
873 sounder data, NGS benchmarks, total station and RTK-GPS survey points.
874 Prepared for the Yuba Accord River Management Team, Marysville, CA.

875 Beechie TJ, Sear DA, Olden JD, Pess GR, Buffington J, Moir H, Roni P, Pollock MM.
876 2010. The next link will exit from NWFSC web site Process-based principles for
877 restoring river ecosystems. *Bioscience* **60** (3): 209-222.

878 Booth AM, Roering JJ, Perron JT, 2009. Automated landslide mapping using spectral
879 analysis and high-resolution topographic data: Puget Sound lowlands,
880 Washington, and Portland Hills, Oregon. *Geomorphology* **109**: 132–147.

881 Brandt SA. 2000. Classification of geomorphological effects downstream of dams.
882 *Catena* **40**: 375-401.

883 Brandtberg T. 2007. Classifying individual tree species under leaf-off and leaf-on
884 conditions using airborne lidar. *ISPRS Journal of Photogrammetry and Remote*
885 *Sensing* **61**: 325-340.

886 Brasington J, Vericat D, Rychkov I. 2012. Modeling riverbed morphology, roughness,
887 and surface sedimentology using high resolution terrestrial laser scanning. *Water*
888 *Resources Research* **48**, W11519.

- 889 Brennan, R., Webster, T.L., 2006. Object-oriented land cover classification of lidar-
890 derived surfaces. *Canadian Journal of Remote Sensing* **32 (2)**: 162-172.
- 891 Brierley, G., Fryirs, K., 2005. Geomorphology and River Management: Applications of
892 the River Styles Framework. Blackwell Publishing, Victoria, Australia (398 pp.).
- 893 Brown RA, Pasternack GB. 2014. Hydrologic and topographic variability modulate
894 channel change in mountain rivers. *Journal of Hydrology* 510: 551-564.
- 895 Brown RA., Pasternack GB., Wallender WW. 2014. Synthetic river valleys: creating
896 prescribed topography for form-process inquiry and river rehabilitation design.
897 *Geomorphology* 214: 40-55. 10.1016/j.geomorph.2014.02.025.
- 898 Buscombe, D. 2016. Spatially explicit spectral analysis of point clouds and geospatial
899 data. *Computers and Geosciences* **86**: 92-108.
- 900 Carley JK, Pasternack GB, Wyrick JR, Barker JR, Bratovich PM, Massa DA, Reedy GD,
901 Johnson TR. 2012. Significant decadal channel change 58-67 years post-dam
902 accounting for uncertainty in topographic change detection between contour
903 maps and point cloud models. *Geomorphology* **179**: 71-88.
- 904 Casas A, Lane SN, Yu D. Benito, G., 2010. A method for parameterising roughness and
905 topographic sub-grid scale effects in hydraulic modelling from LiDAR data.
906 *Hydrology and Earth System Sciences* **14**: 1567-1579.
- 907 Das T, Dettinger M, Cayan D, Hidalgo H, 2011, Potential increase in floods in
908 California's Sierra Nevada under future climate projections. *Climatic Change* **109**
909 **(Suppl 1)**: 71-94.
- 910 Drăguț L, Eisank C. 2011. Object representations at multiple scales from digital
911 elevation models. *Geomorphology* **129 (3-4)**: 183-189.
- 912 Evans IS. 2012. Geomorphometry and landform mapping: What is a landform?
913 *Geomorphology* **137**:94-106.
- 914 Ferguson RI, Ashworth PJ. 1992. Spatial patterns of bedload transport and channel
915 change in braided and near-braided rivers. In: Billi P, Hey RD, Thorne CR,
916 Tacconi P (eds.) *Dynamics of gravel bed rivers*, Wiley, Chichester, p. 477-496.
- 917 Fonstad, MA, Dietrich JT, Courville BC, Jensen JL, Carbonneau PE. 2013. Topographic
918 structure from motion: a new development in photogrammetric measurement.
919 *Earth Surface Processes and Landforms* **38 (4)**: 421-430.

- 920 Frissell CA, Liss WJ, Warren CE, Hurley MD. 1986. A hierarchical framework for stream
921 habitat classification: Viewing streams in a watershed context. *Environmental*
922 *Management* 10: 199-214. DOI: 10.1007/bf01867358.
- 923 Fuller IC, Large ARG, Charlton ME, Heritage GL, Milan DJ. 2003. Reach-scale
924 sediment transfers: an evaluation of two morphological budgeting approaches.
925 *Earth Surface Processes and Landforms* 28: 889-903.
- 926 Gangodagamage C, Barnes E, Foufoulageorgiou E. 2007. Scaling in river corridor
927 widths depicts organization in valley morphology. *Geomorphology* 91 (3): 198-
928 215.
- 929 Gilbert GK. 1917. Hydraulic-mining debris in the Sierra Nevada. US Geological Survey
930 Professional Paper 105, Washington DC.
- 931 Glennie CL, Carter WE, Shrestha RL, Dietrich WE. 2013. Geodetic imaging with
932 airborne LiDAR: the Earth's surface revealed. *Reports on Progress in Physics* 76
933 (8): 086801.
- 934 Grant GE, Schmidt JC, Lewis SL. 2003. A Geological Framework for Interpreting
935 Downstream Effects of Dams on Rivers. In *A Peculiar River*, O'Connor JE, Grant
936 GE (eds). American Geophysical Union: Washington, D.C.; 209-223.
- 937 Grant, G.E., Swanson, F.J., Wolman, M.G., 1990. Pattern and origin of stepped-bed
938 morphology in high-gradient streams, Western Cascades, Oregon. *Geological*
939 *Society of America Bulletin* 102: 340-352.
- 940 Hack JT. 1960. Interpretation of Erosional Topography in Humid Temperate Regions.
941 *American Journal of Science*, Bradley Volume, Vol 258-A, p. 80-97.
- 942 Hadley RF, Schumm SA. 1961. Sediment sources and drainage basin characteristics in
943 Upper Cheyenne River Basin. USGS Water-Supply Paper 1531-B.
- 944 Hauer, C., Mandlbürger, G., Habersack, H., 2009. Hydraulically related
945 hydromorphological units: description based on a new conceptual mesohabitat
946 evaluation model (MEM) using LiDAR data as geometric input. *River Res. Appl.*
947 25, 29–47.
- 948 Hay GJ, Marceau DJ, Dubè P, Bouchard A, 2001. A multiscale framework for landscape
949 analysis: object-specific analysis and upscaling. *Landscape Ecology* 16: 471-
950 490.
- 951 Heritage GL, Milan DJ, Large RG, Fuller IC. 2009. Influence of survey strategy and
952 interpolation model on DEM quality. *Geomorphology* 112: 334-344.

- 953 Horne GS, Patton PC. 1989. Bedload-sediment transport through the Connecticut River
954 estuary. *Geological Society of America Bulletin* **101 (6)**: 805-819.
- 955 James LA. 2005. Sediment from hydraulic mining detained by Englebright and small
956 dams in the Yuba basin. *Geomorphology* 71: 202-226. DOI:
957 10.1016/j.geomorph.2004.02.016
- 958 James LA, Hodgson ME, Ghoshal S, Latiolais MM. 2010. Geomorphic change detection
959 using historic maps and DEM differencing: the temporal dimension of geospatial
960 analysis. *Geomorphology* **137 (1)**: 181-198.
- 961 James LA, Singer MB, Ghoshal S, Megison M. 2009. Historical channel changes in the
962 lower Yuba and Feather Rivers, California: long-term effects of contrasting river-
963 management strategies. In *Management and Restoration of Fluvial Systems with
964 Broad Historical Changes and Human Impacts*, James LA, Rathburn SL,
965 Whittecar GR (eds). Geological Society of America Special Paper 451: 57–81.
966 DOI:10.1130/2008.2451(04).
- 967 Lashermes B, Foufoula-Georgiou E, Dietrich WE. 2007. Channel network extraction
968 from high resolution topography using wavelets. *Geophysical Research Letters*
969 **34**: L23S04. <http://dx.doi.org/10.1029/2007GL031140>.
- 970 Lawler DM. 1993. The measurement of river bank erosion and lateral channel change:
971 A review. *Earth Surface Processes and Landforms* **18 (9)**: 777-821.
- 972 Legleiter CJ, Kyriakidis PC. 2008. Spatial prediction of river channel topography by
973 kriging. *Earth Surface Processes and Landforms* **33**: 841-867. doi:
974 10.1002/esp.1579.
- 975 Leopold LB, Reed H, Miller A. 2005. Geomorphic Effects of Urbanization in Forty-One
976 Years of Observation. *Proceedings of the American Philosophical Society* **149**
977 **(3)**: 349-371.
- 978 Lindsay JB, Ashmore PE. 2002. The effects of survey frequency on estimates of scour
979 and fill in a braided river model. *Earth Surface Processes and Landforms* 27: 27-
980 43
- 981 Mandlbürger G, Hauer C, Wieser M, Pfeifer N. 2015. Topo-bathymetric LiDAR for
982 monitoring river morphodynamics and instream habitats- a case study at the
983 Pielach River. *Remote Sensing* **7 (5)**: 6160-6195.
- 984 Marquis GA, Roy AG. 2012. Using multiple bed load measurements: Toward the
985 identification of bed dilation and contraction in gravel-bed rivers. *Journal of*

- 986 Geophysical Research: Earth Surface 117: n/a-n/a. DOI:
987 10.1029/2011JF002120.
- 988 Merz JE, Pasternack GB, Wheaton JM. 2006. Sediment budget for salmonid spawning
989 habitat rehabilitation in the Mokelumne River. *Geomorphology* **76 (1-2)**: 207-228.
- 990 Milan, DJ, Heritage GL, Large ARG, Entwistle NS. 2010. Mapping hydraulic biotopes
991 using terrestrial laser scan data of water surface properties. *Earth Surface*
992 *Processes and Landforms* **35**: 918-931.
- 993 Milan DJ, Hetherington D, Heritage GL. 2007. Application of a 3D laser scanner in the
994 assessment of erosion and deposition volumes in a proglacial river. *Earth*
995 *Surface Processes and Landforms* **32**: 1657-1674.
- 996 Nelson PA, Bellugi D., Dietrich WE. 2014. Delineation of river bed-surface patches by
997 clustering high-resolution spatial grain size data. *Geomorphology* **205**: 102-119.
- 998 Parker G, Toro-Escobar CM, Ramey M, Beck S. 2003. The effect of floodwater
999 extraction on the morphology of mountain streams. *Journal of Hydraulic*
1000 *Engineering* **129 (11)**: 885-895.
- 1001 Passalacqua P, Belmont P, Staley DM, Simley JD, Arrowsmith JR, Bode CA, Crosby C,
1002 DeLong SB, Glenn NF, Kelly SA, Lague D, Sangireddy H, Schaffrath K, Tarboton
1003 DG, Wasklewicz T, Wheaton JM. 2015. Analyzing high resolution topography for
1004 advancing the understanding of mass and energy transfer through landscapes: a
1005 review. *Earth Sci. Rev.* 148, 174–193.
1006 <http://dx.doi.org/10.1016/j.earscirev.2015.05.012>.
- 1007 Pasternack GB. 2008. SHIRA-based river analysis and field-based manipulative
1008 sediment transport experiments to balance habitat and geomorphic goals on the
1009 Lower Yuba River. Cooperative Ecosystems Studies Unit (CESU) 81332 6 J002
1010 Final Report: University of California at Davis, Davis, CA.
- 1011 Pasternack GB. 2011. 2D Modeling and Ecohydraulic Analysis. Createspace: Seattle,
1012 WA, USA.
- 1013 Pasternack GB., Brush GS., Hilgartner WB. 2001. Impact of historic land-use change on
1014 sediment delivery to a Chesapeake Bay subestuarine delta. *Earth Surface*
1015 *processes and Landforms* 26:409-427.
- 1016 Perron JT, Kirchner JW, Dietrich WE. 2008. Spectral signatures of characteristic spatial
1017 scales and nonfractal structure in landscapes. *Journal of Geophysical Research-*
1018 *Earth Surface* **113**: F04003.

- 1019 Sawyer AM, Pasternack GB, Moir HJ, Fulton AA. 2010. Riffle-pool maintenance and
1020 flow convergence routing confirmed on a large gravel bed river. *Geomorphology*
1021 **114**: 143-160.
- 1022 Schaffrath KR, Belmont, P, Wheaton JM. 2015. Landscape-scale geomorphic change
1023 detection: Quantifying spatially variable uncertainty and circumventing legacy
1024 data issues. *Geomorphology* **250**: 334-348.
- 1025 Sear DA. 1994. River restoration and geomorphology. *Aquatic Conservation* **4**: 169-177.
- 1026 Singer MB, Aalto, R, James LA, Kilham NE, Higson JL, Ghoshal S. 2013. Enduring
1027 legacy of a toxic fan via episodic redistribution of California gold mining debris.
1028 *Proceedings of the National Academy of Sciences* **110 (46)**: 18436-18441.
- 1029 Storer TI, Usinger RL, Lukas D. 2004. Sierra Nevada Natural History (revised ed.).
1030 University of California Press: Berkeley, CA, USA.
- 1031 Tarolli P. 2014. High-resolution topography for understanding Earth surface processes:
1032 Opportunities and challenges. *Geomorphology* **216**: 295-312.
- 1033 Tarolli P, Tarboton DG. 2006. A new method for determination of most likely landslide
1034 initiation points and the evaluation of digital terrain model scale in terrain stability
1035 mapping. *Hydrology and Earth System Sciences* **10**: 663-677.
- 1036 Thorne, CR. 1998. Stream Reconnaissance Guidebook: Geomorphological
1037 Investigation and Analysis of River Channels, John Wiley & Sons, Chichester,
1038 UK.
- 1039 Trimble SW, Weirich FH, Hoag BL. 1987. Reforestation and the reduction of water yield
1040 on the Southern Piedmont since circa 1940, *Water Resources Research* **23 (3)**:
1041 425-437, doi:10.1029/WR023i003p00425.
- 1042 Tucker GE, Slingerland R. 1997. Drainage basin responses to climate change. *Water*
1043 *Resources Research* **33 (8)**: 2031-2047
- 1044 Valle B, Pasternack G. 2006. Field mapping and digital elevation modelling of
1045 submerged and unsubmerged hydraulic jump regions in a bedrock step-pool
1046 channel. *Earth Surface Processes and Landforms*, **31 (6)**: 646-664.
- 1047 Wadeson RA. 1994. A geomorphological approach to the identification and
1048 classification of instream flow environments. *Southern African Journal of Aquatic*
1049 *Sciences* **20**: 38-61. DOI: 10.1080/10183469.1994.9631349

- 1050 Warrick JA, Rubin DM. 2007. Suspended-sediment rating curve response to
1051 urbanization and wildfire, Santa Ana River, California. *Journal of Geophysical*
1052 *Research* **112**: F02018.
- 1053 Wheaton JM, Brasington J, Darby SE, Sear D. 2010a. Accounting for uncertainty in
1054 DEMs from repeat topographic surveys: improved sediment budgets. *Earth*
1055 *Surface Processes and Landforms* **35** (2): 136-156.
- 1056 Wheaton JM, Brasington J, Darby S, Merz JE, Pasternack GB, Sear DA, Vericat D.
1057 2010b. Linking geomorphic changes to salmonid habitat at a scale relevant to
1058 fish. *River Research and Applications* **26**: 469-486.
- 1059 Wheaton JM, Brasington J, Darby SE, Kasprak A, Sear D, Vericat D. 2013.
1060 Morphodynamic signatures of braiding mechanisms as expressed through
1061 change in sediment storage in a gravel-bed river. *Journal of Geophysical*
1062 *Research: Earth Surface* **118** (2): 759-779.
- 1063 Wheaton JM, Fryirs KA, Brierley G, Bangen SG, Bouwes N, O'Brien G. 2015.
1064 Geomorphic mapping and taxonomy of fluvial landforms. *Geomorphology* 248:
1065 273-295. DOI: <http://dx.doi.org/10.1016/j.geomorph.2015.07.010>
- 1066 White JQ, Pasternack GB, Moir HJ. 2010. Valley width variation influences riffle-pool
1067 location and persistence on a rapidly incising gravel-bed river. *Geomorphology*
1068 **121**: 206-221.
- 1069 Williams GP, Wolman MG. 1984. Downstream effects of dams on alluvial rivers. U.S.
1070 Geological Survey Professional Paper 1286.
- 1071 Williams RD, Measures R, Hicks M, Brasington J. 2016. Assessment of a numerical
1072 model to reproduce event-scale erosion and deposition distributions in a braided
1073 river. *Water Resources Research*: n/a-n/a. DOI: 10.1002/2015WR018491
- 1074 Wyrick JR, Pasternack GB. 2012. Landforms of the Lower Yuba River. Prepared for the
1075 Yuba Accord River Management Team. University of California, Davis, CA.
- 1076 Wyrick JR, Pasternack GB. 2015. Revealing the natural complexity of topographic
1077 change processes through repeat surveys and decision-tree classification. *Earth*
1078 *Surface Processes and Landforms*, doi: 10.1002/esp.3854
- 1079 Wyrick JR, Senter AE, Pasternack GB. 2014. Revealing the natural complexity of fluvial
1080 morphology through 2D hydrodynamic delineation of river landforms.
1081 *Geomorphology* **210**: 14-22.
- 1082 Wyrick JR, Pasternack GB. 2014. Geospatial organization of fluvial landforms in a
1083 gravel-cobble river: beyond the riffle-pool couplet. *Geomorphology* **213**: 48-65.

1084 Zhang W, Montgomery D, 1994. Digital elevation model grid size, landscape
1085 representation and hydrologic simulations. *Water Resources Research* **30**: 1019-
1086 1028.
1087

Uncorrected final

Table 1. Hydraulic, geomorphic, and topographic change metrics for the reaches of the lower Yuba River.

Reach	Valley Width (m)						Floodway wetted area (m ²)	Bankfull wetted area (m ²)	Floodway wetted area (m ²)	Tributary inflow?	Thalweg length (m)	Valley centerline length (m)
	Mean Baseflow* Width (m)	Mean Bankfull* Width (m)	Mean Floodway* Width (m)	min	mean	max						
Englebright Dam*	36.6	51.5	72.2	55.5	94.8	175.6	24186	62654	no	1259	1217	
Narrows*	-	-	-	49.4	90.8	181.7	-	-	yes	2044	1859	
Timbuctoo Bend	62.5	84.4	134.4	96.9	165.8	411.2	285203	480109	no	6337	5766	
Parks Bar	60.7	96.3	206.7	94.8	297.5	434.0	772746	665885	no	7919	6920	
Dry Creek	75.6	130.1	263.7	238.7	307.5	489.8	483367	458149	yes	3799	3579	
DPD	60.0	119.8	313.3	198.4	448.7	554.1	955056	585155	no	5639	4974	
Hallwood	55.8	102.1	210.9	70.7	271.0	569.1	809597	766540	no	8382	7785	
Marysville	53.0	70.4	115.5	68.3	171.3	381.3	192730	336449	no	5334	5005	

(B) Geomorphic classification metrics

Reach	Entrenchment Ratio	Width/Depth Ratio	Sinuosity	Slope	Substrate (mm)	Substrate Class	Rosgen (1996) classification	Spec Strm Power W/m ²	Fr _b	S/Fr _b
Englebright Dam	1.62	31.3	1.04	0.0031	298	small boulder	B2c	83.7	0.25	0.0124
Narrows	-	-	-	-	-	-	-	-	-	-
Timbuctoo Bend	2.12	82.4	1.10	0.0020	164	large cobble	B3c	33.1	0.36	0.0056
Parks Bar	2.93	107.9	1.14	0.0019	117	small cobble	C3	27.2	0.31	0.0061
Dry Creek	2.45	122.3	1.06	0.0014	87	small cobble	C3	14.4	0.25	0.0054
DPD	3.54	85.4	1.13	0.0018	87	small cobble	C3	20.4	0.25	0.0071
Hallwood	2.61	70.8	1.08	0.0013	61	coarse gravel	C4	17.8	0.22	0.0060
Marysville	2.61	23.1	1.07	0.0005	40	coarse gravel	C4c-	10.3	0.15	0.0034

(C) Topographic change metrics. Negative numbers indicate scour.

Reach	Scour Area (%)	Fill Area (%)	Mean rate in		Mean net rate (cm/yr)
			scour areas (cm/yr)	fill areas (cm/yr)	
Englebright Dam	-	-	-	-	-
Narrows	-	-	-	-	-
Timbuctoo Bend	44.5	10.4	-13.6	14.7	-4.5
Parks Bar	19.7	32.9	-13.9	8.7	0.1
Dry Creek	55.3	12.8	-13.0	10.1	-5.9
DPD	12.0	44.9	-17.3	8.9	1.9
Hallwood	11.0	34.9	-12.7	8.6	1.6
Marysville	22.9	24.8	-10.8	10.3	0.1

*Englebright Dam and Narrows Reaches were not investigated in this study, but their data are included for completeness.

1088 Figure Captions

1089

1090 Fig. 1. Location map of the lower Yuba River segment within its catchment and in
1091 California.

1092

1093 Fig. 2. Inundation area maps of the lower Yuba River. Black is the inundation area for a
1094 flow of $109 \text{ m}^3/\text{s}$ and grey shows the alluvial valley area used in the DEM
1095 difference analysis. White voids in the valley are areas where there were
1096 topographic survey gaps in the 1999 DEM. Dashed double lines perpendicular to
1097 the river are geomorphic reach breaks.

1098

1099 Fig. 3. Workflow for creating DEM difference raster using methodology from Carley et
1100 al. (2012)

1101

1102 Fig. 4. Patterns of scour (red), fill (blue), no change (cream), and no data (white) in river
1103 reaches (black) for the epoch from 1999 to 2006-2008.

1104

1105 Fig. 5. Morphological unit example maps illustrating how different the assemblages are
1106 between reaches.

1107

1108 Fig. 6. Longitudinal profile of the percent area of scour, fill, and no change across the
1109 river valley at each centerline station for the epoch from 1999 to 2006-2008.

1110

1111 Fig. 7. Annualized sediment budget rates at the reach scales ($10^4 \text{ m}^3/\text{yr}$). Dark grey
1112 horizontal arrows with dashed outline denote scour volumes and light grey
1113 vertical arrows with solid outline denote fill.

1114

1115 Fig. 8. Reach-scale regressions between geomorphic controls and topographic change
1116 metrics. Note that deeper scour corresponds with more negative values.

1117

1118 Fig. 9. Topographic change maps for two small parts of contrasting reaches, (A) DPD
1119 and (B) Marysville. The former shows lateral migration relative to the 1999
1120 channel boundary (thick black line) with intense scour (red) just outside the
1121 channel at outer banks and deposition (blue) inside the channel. The latter shows
1122 in-channel downcutting and overbank deposition.

1123

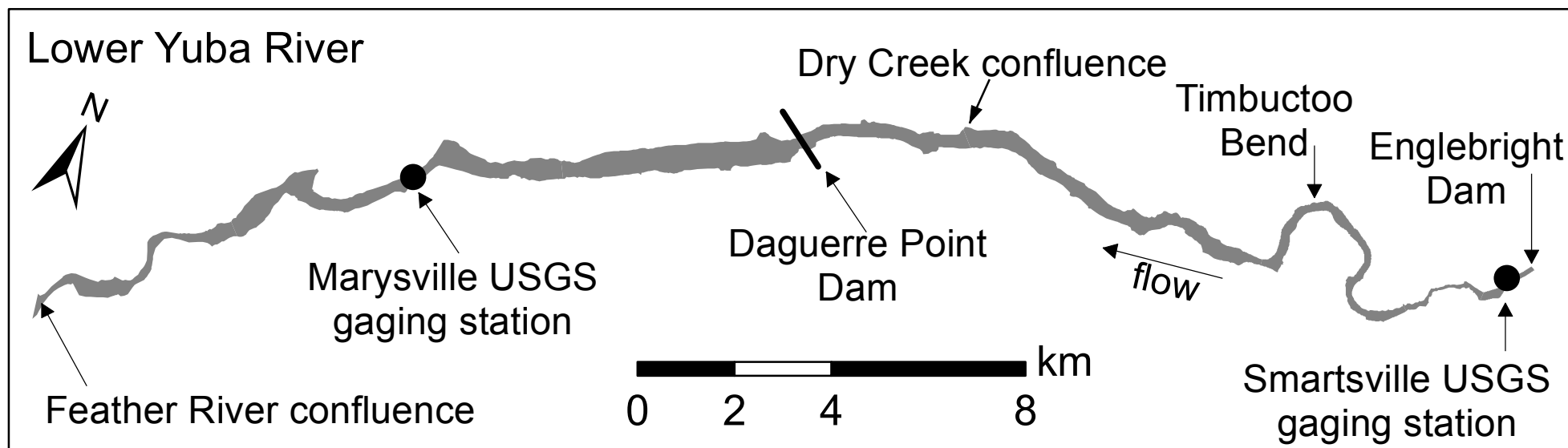
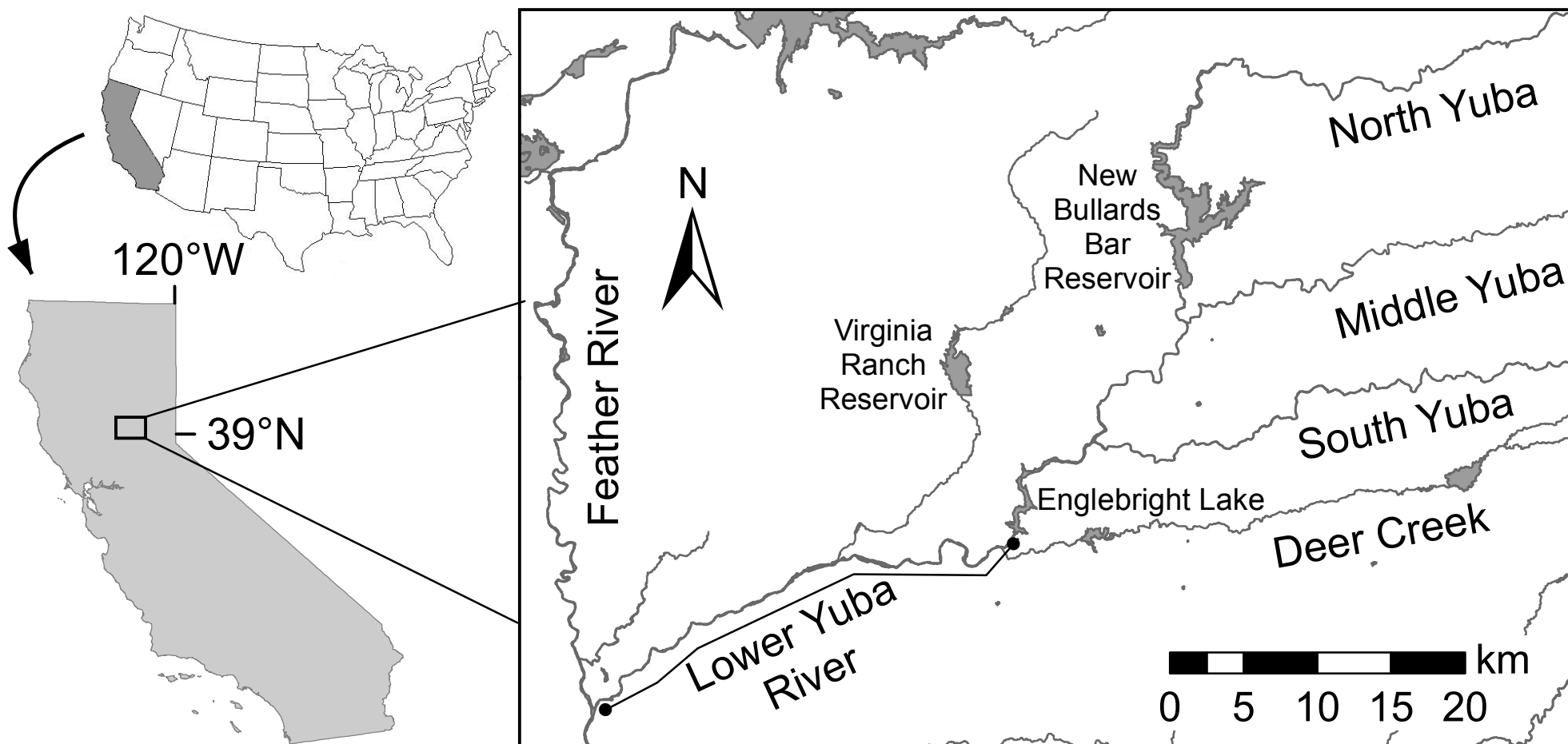
1124 Fig. 10. Net volumetric change in morphologic units, sorted from most depositional to
1125 most erosional. These are the changes that caused the MUs to be formed.

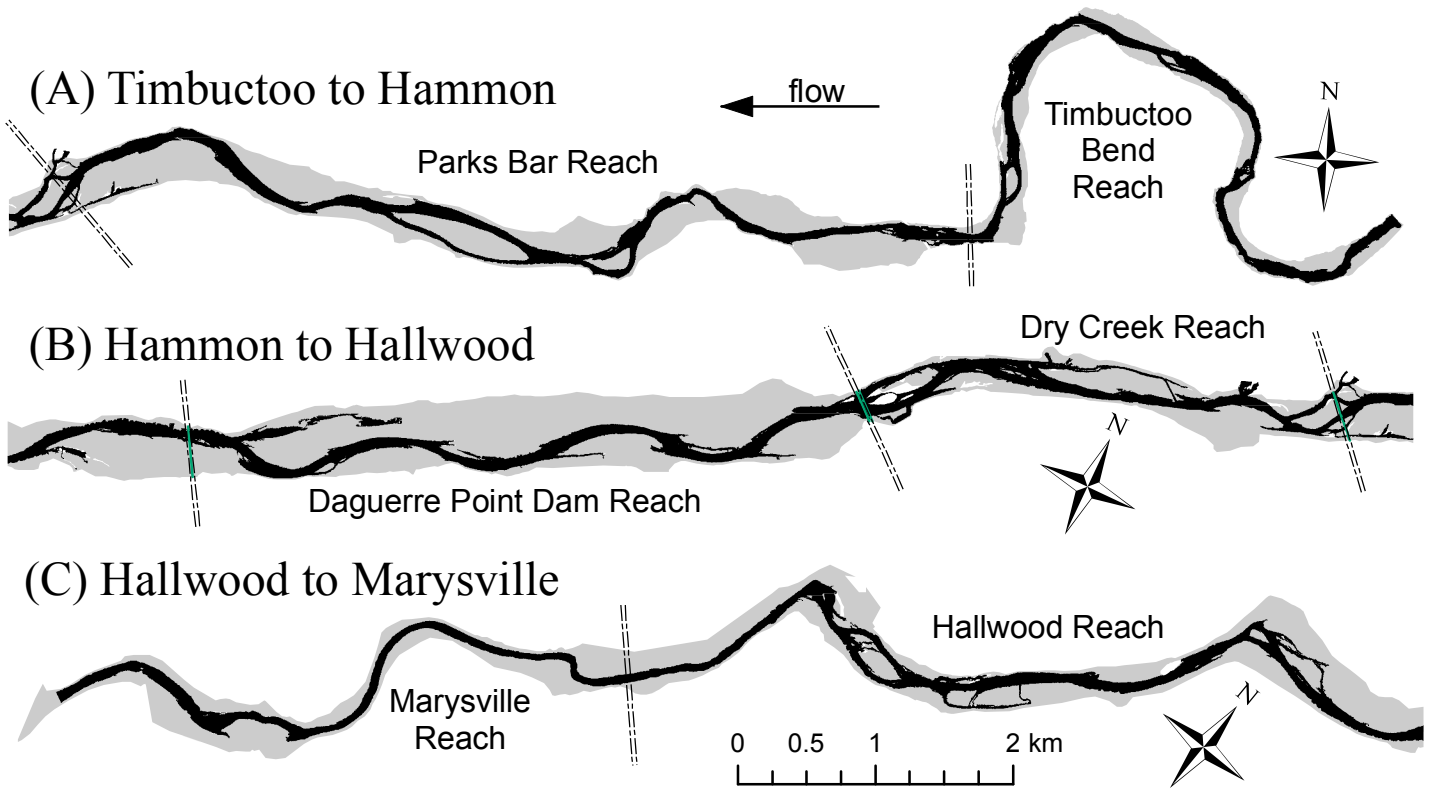
1126

1127 Fig. 11. Mean rates of elevation change for the morphological unit types as mapped at
1128 the end of the study epoch. These are the changes that caused the units to be
1129 formed.

1130

Uncorrected final





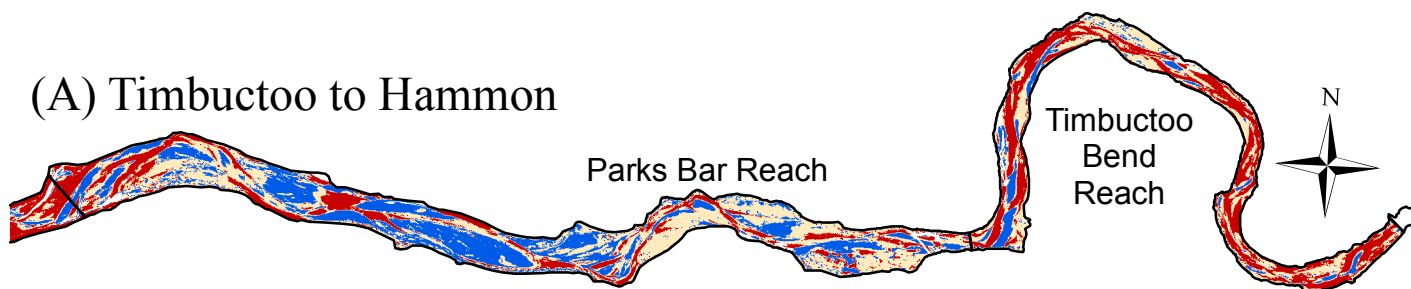
Topographic change detection workflow

- a. Create a uniform {x,y} point grid with 0.3 m point spacing.
- b. Elevate the 0.3 m point grid using the topographic data for each map to create oversampled topographic point datasets for {x,y,z}_{time1} and {x,y,z}_{time2} that capture all available topographic information in the source DEMs.
- c. For each 0.3 m {x,y,z} topographic dataset, create a raster of standard deviation (SD) of point elevation with a 1.5 x 1.5 m cell size (yielding 25 points per cell in the statistical computation).
- d. Apply the appropriate survey and instrument error (SIE) empirical equation from Heritage *et al.* (2009) to the SD rasters to obtain the SIE raster for each topographic map.
- e. Produce a Level of Detection (LoD) grid that combines the two SIE rasters into a single error raster using the t-value for 95 % confidence (1.96) and the statistical equation for error propagation given by:

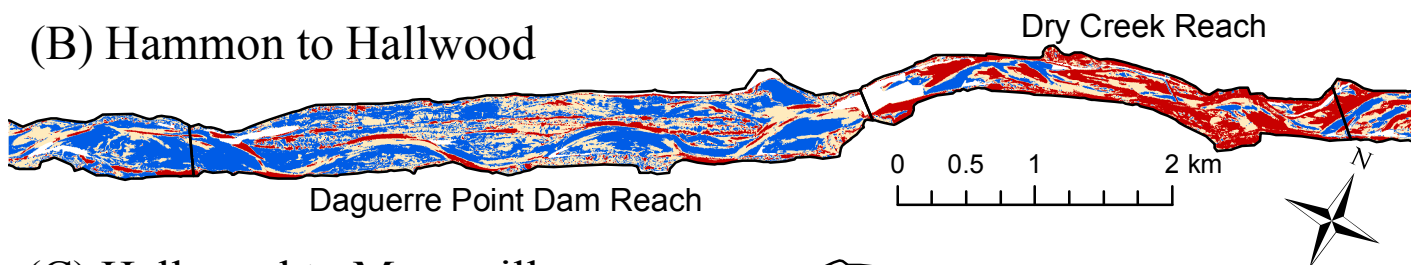
$$LoD = t\sqrt{(SIE_{time1})^2 + (SIE_{time2})^2}$$

- f. Create the raw DoD raster with a 1.5 x 1.5 m cell size.
- g. Create separate deposition and erosion rasters using the “Con” function in the ArcGIS raster calculator.
- h. Remove the LoD from each raster by subtracting it from the deposition-only raw DoD and adding it to the erosion-only raw DoD.

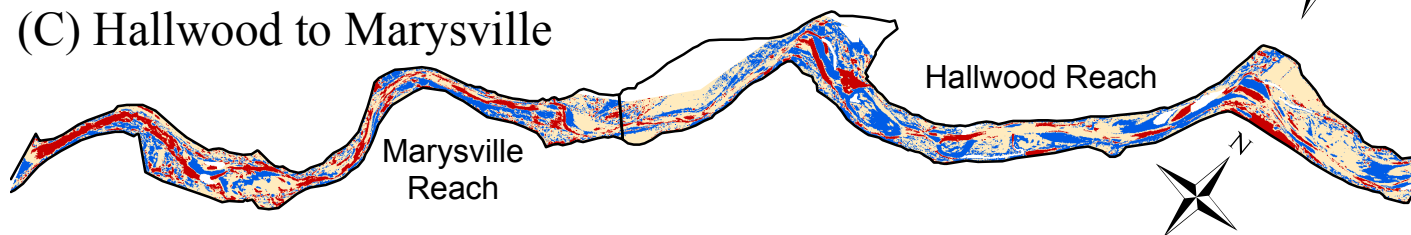
(A) Timbuctoo to Hammon

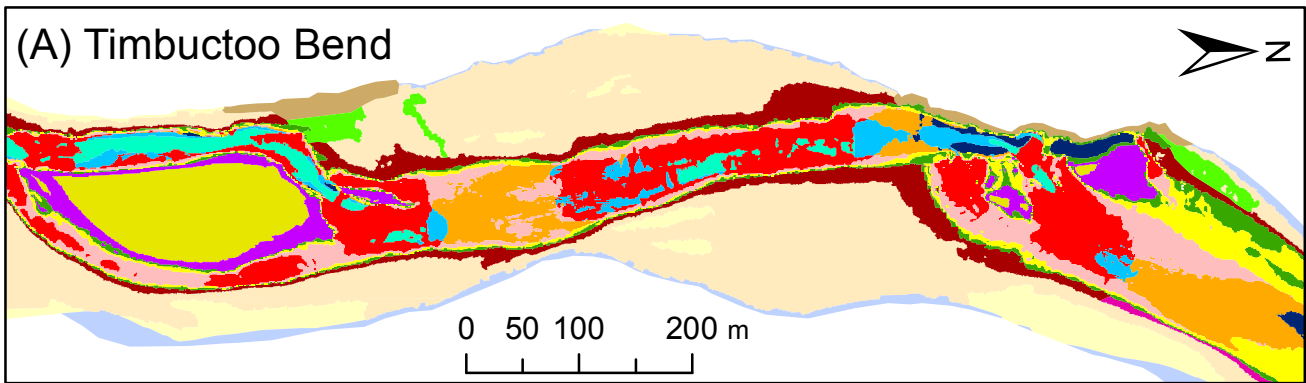


(B) Hammon to Hallwood

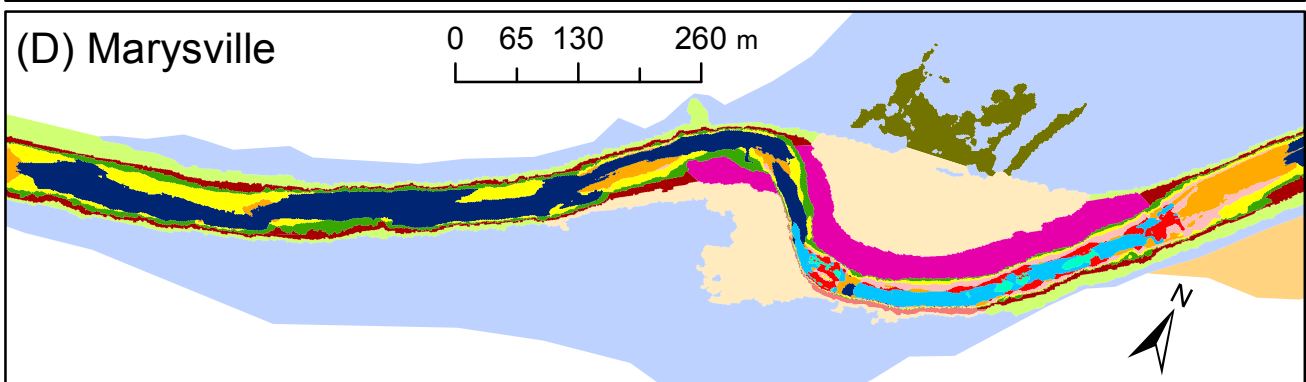
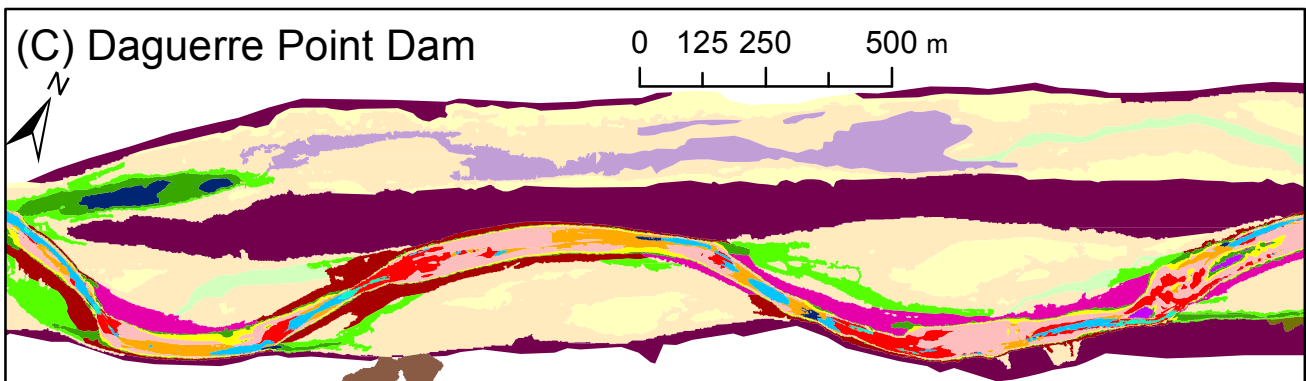
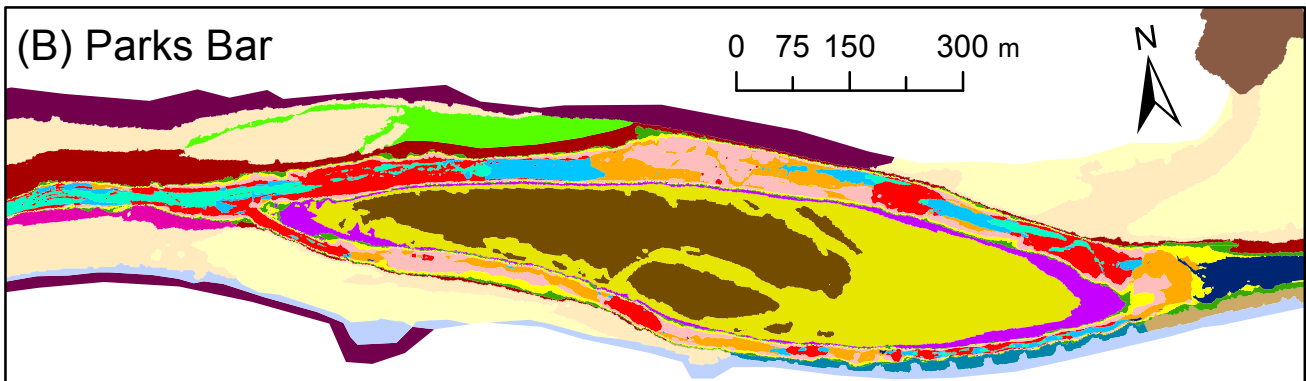


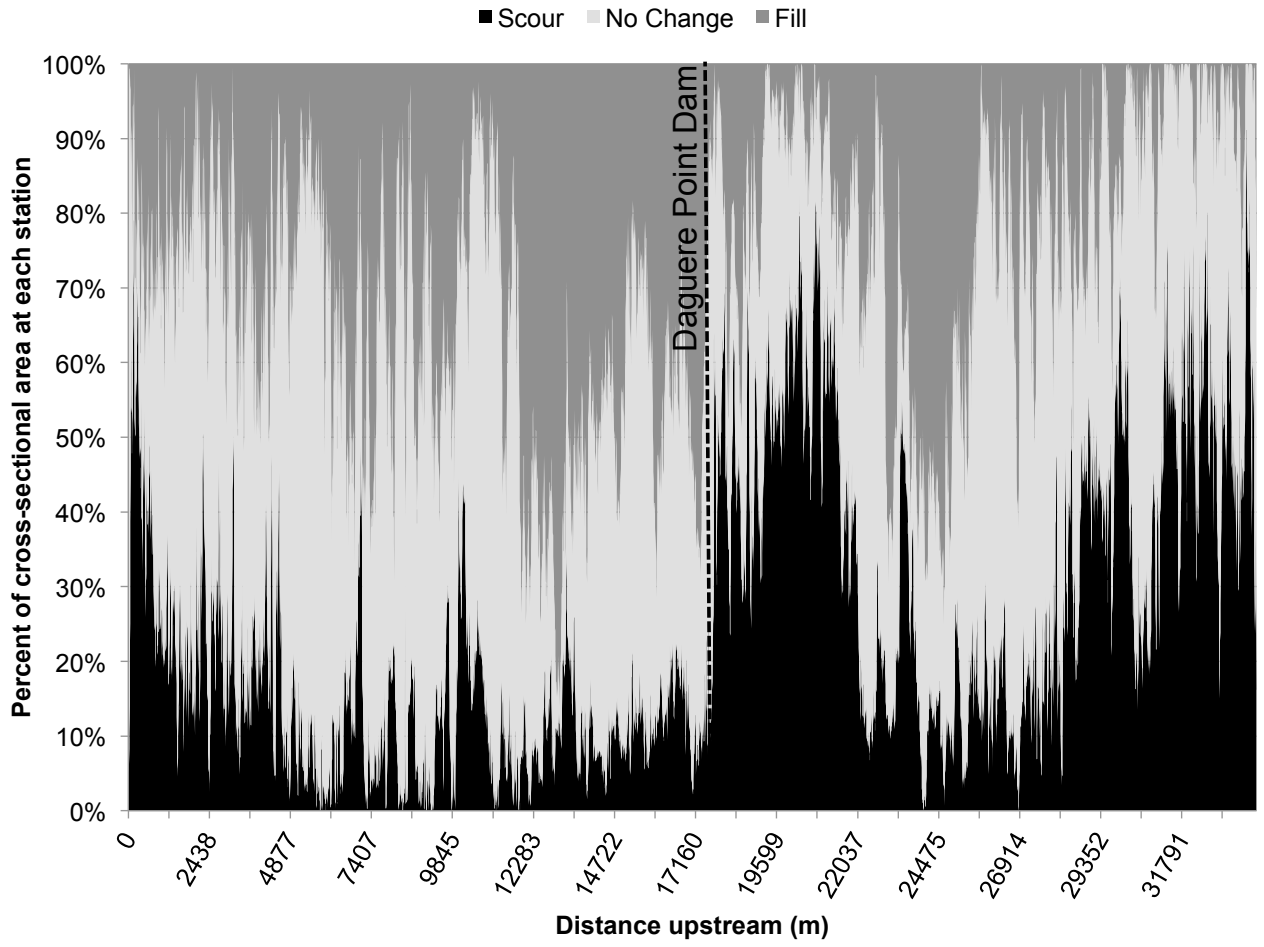
(C) Hallwood to Marysville

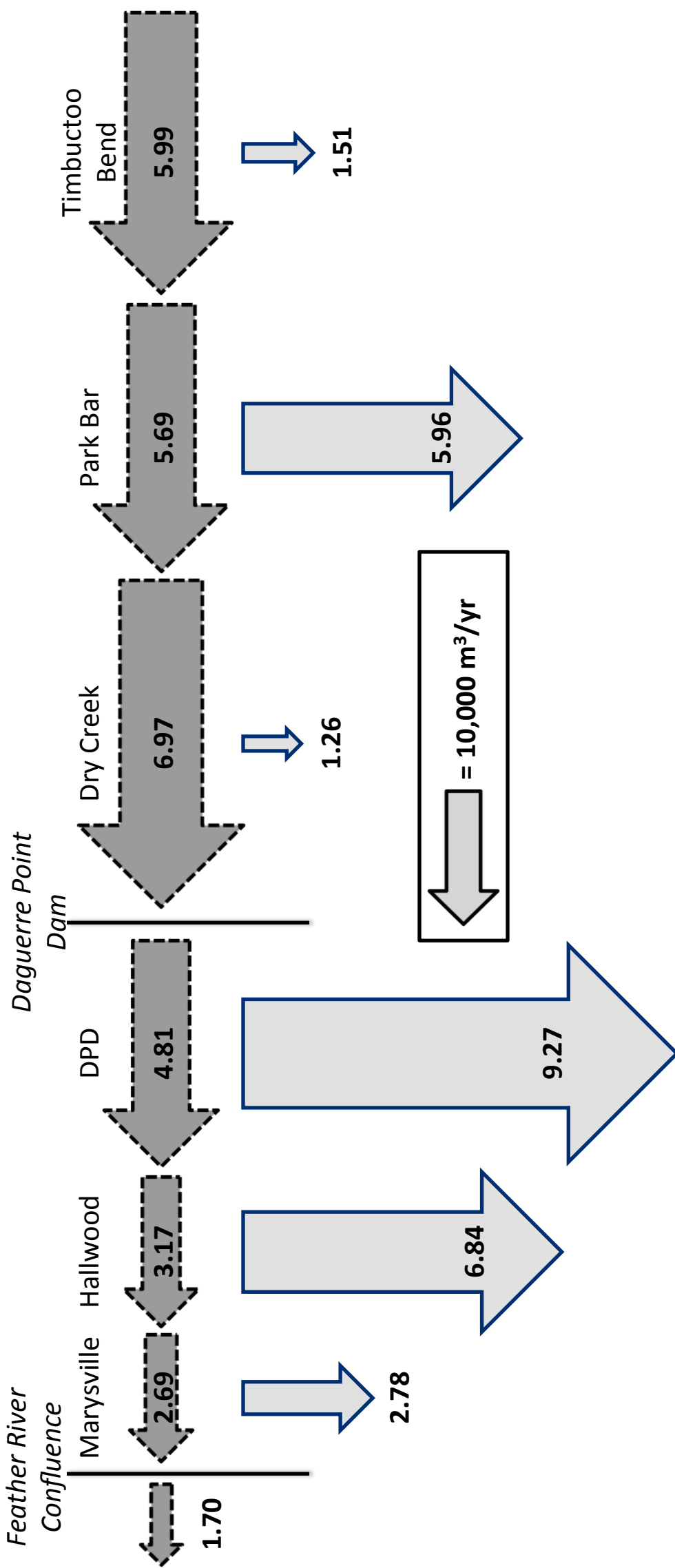


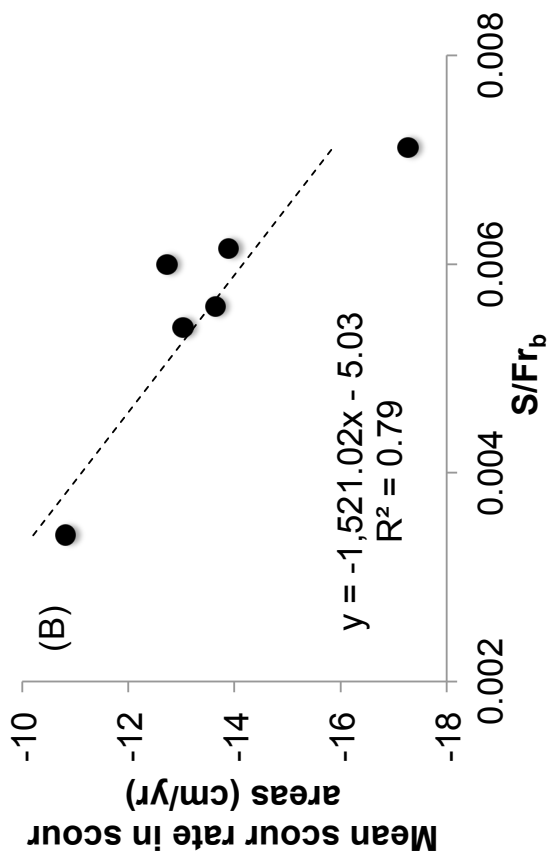
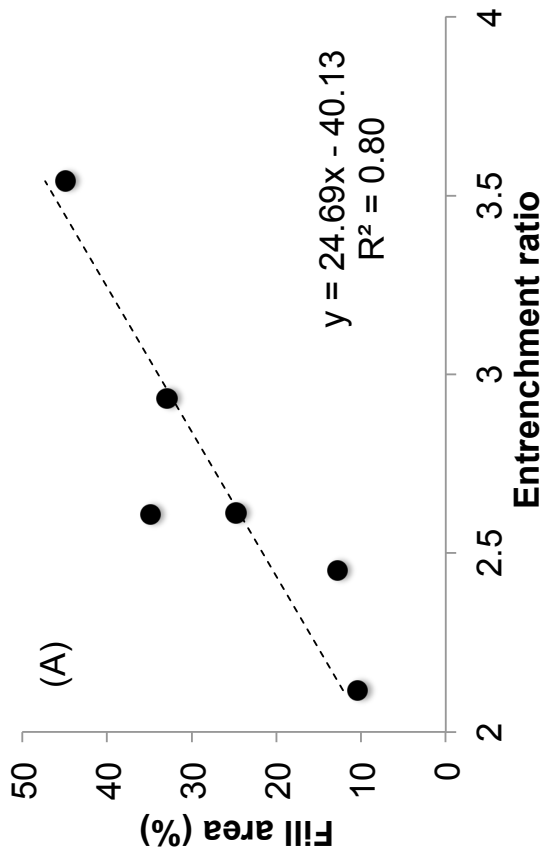


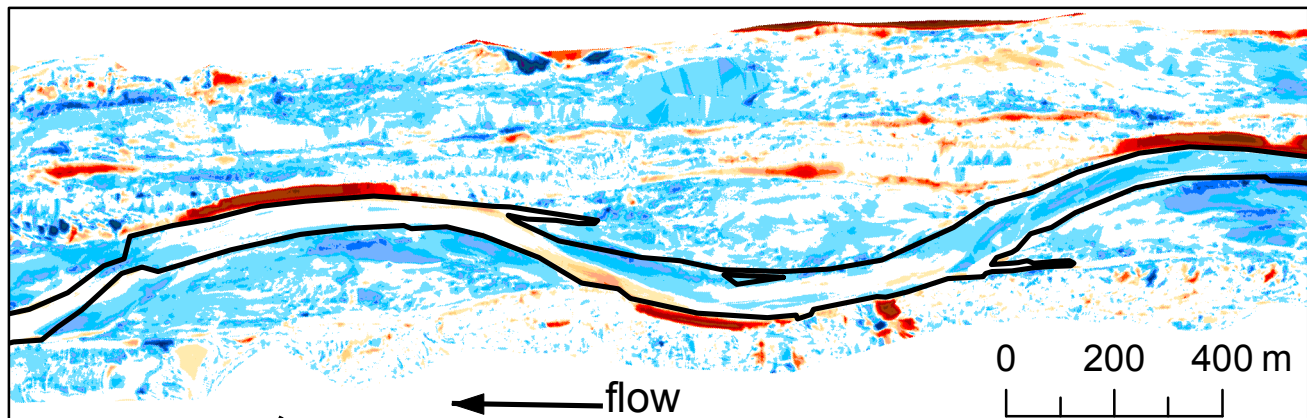
- | | | | | |
|---------------------|------------------------|-------------|-------------------|-------------------|
| morphological units | fast glide | lateral bar | riffle | tailings |
| agriplain | flood runner | levee | riffle transition | terrace |
| backswamp | floodplain | medial bar | run | tributary channel |
| bank | high floodplain | mining pit | slackwater | tributary delta |
| bridge pier | hillside/bedrock | point bar | slow glide | |
| chute | island high floodplain | pond | spur dike | |
| cutbank | island-floodplain | pool | swale | |
- ← flow



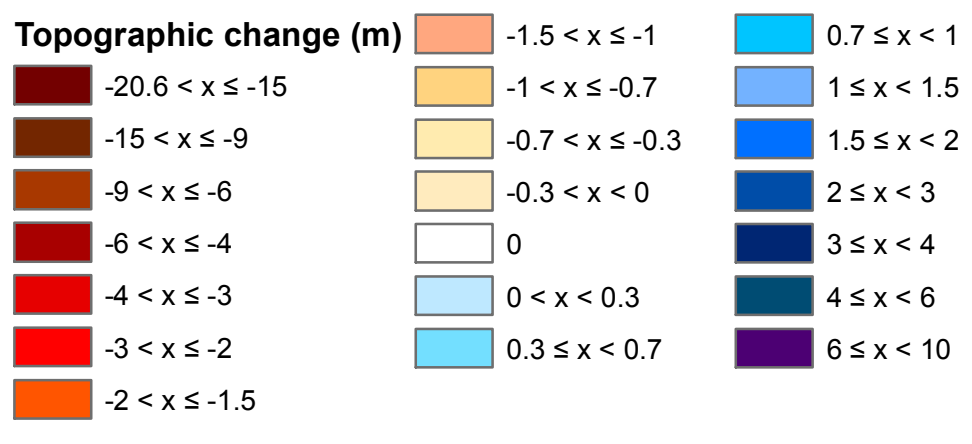





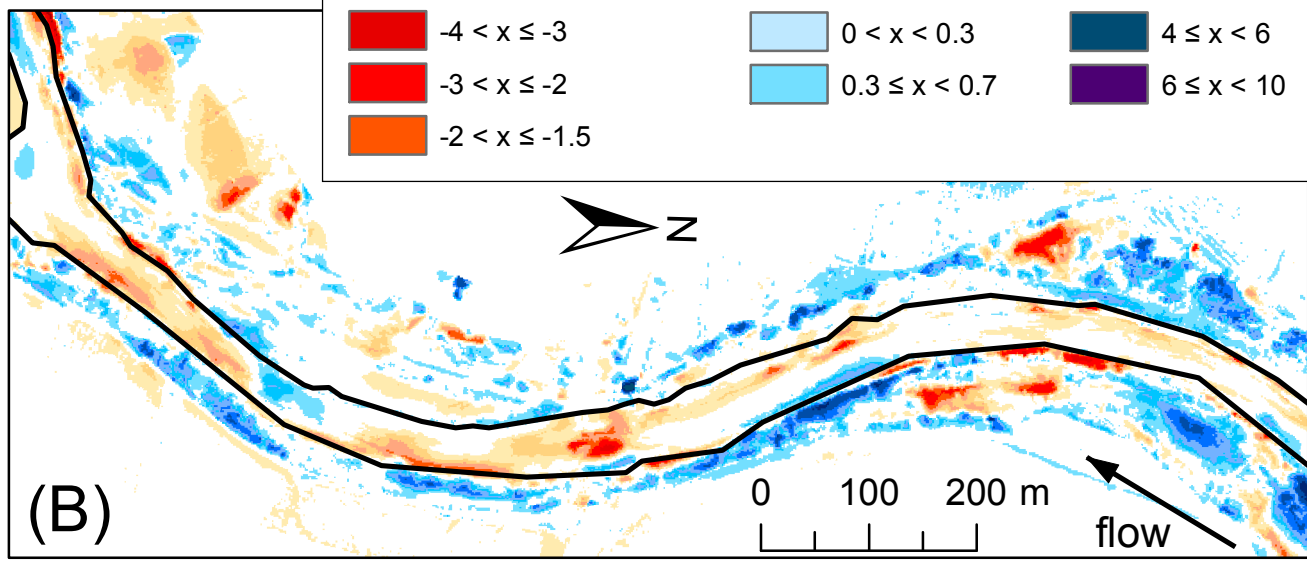




(A)



 1999 channel



(B)



